the brain that can differentiate into neurons, oligodendrocytes, and astrocytes *in vitro*. Marrow stromal cells have been shown to possess many characteristics of mesenchymal stem cells (Prockop, 1997), and pluripotent progenitor marrow stromal cells can differentiate into various types of cell types, including osteoblasts (Rickard et al., 1994; Friedenstein et al., 1987), myocytes (Ferrari et al., 1998), adipocytes, tenocytes, and chondroblasts (Ashton et al., 1980). We recently reported the differentiation of mesenchymal stem cells into cardiomyocytes after exposure to 5-azacytidine and the establishment of cell line CMG (*cardiomyogenic*) that differentiates into cardiomyocytes *in vitro* (Makino et al., 1999). CMG cells exhibit spontaneous beating and express atrial natriuretic peptide (ANP) and brain natriuretic peptide (BNP), and they may provide a useful and powerful tool for cardiomyocyte transplantation after further characterization of their cardiomyocyte phenotype.

This paper describes the characteristics of bone marrow-derived regenerated cardiomyocytes and discusses the possibility of using them for cardiovascular tissue engineering. The expression and function of adrenergic and muscarinic receptors in CMG cells is also described, because these receptors play a critical role in modulating cardiac function (Hakuno et al., 2002).

Mesenchymal marrow stem cells as a possible source of cardiomyocytes: The cardiomyogenic (CMG) cell?

Figure 1 shows the classification of the stem cell system of adults (Fukuda, 2001). Bone marrow stromal cells were previously used as a feeder layer to culture hematopoietic stem cells, and are known to be of mesodermal origin and produce various cytokines and growth factors. In late 1990's, a number of papers reported that bone marrow stromal cells contain multipotent stem cells for non-hematopoietic tissues, called 'marrow mesenchymal stem cells', that could differentiate into osteoblasts, chondroblasts, and adipocytes. All of these cells were known to be of mesodermal origin. If mesenchymal stem cells are multipotent, we hypothesized that they might have the ability to differentiate into cardiomyocytes and instituted this study. We also thought that bone marrow cells could be obtained from patients themselves and that autologous cells would not be rejected after cell transplantation.

Method of establishing bone-marrow derived cardiomyocytes

Female C3H/He mice were anesthetized with ether, their femora were excised, and primary culture of the marrow cells was performed according to Dexter's method. Cells were cultured in Iscove's modified Dulbecco's medium (IMDM) supplemented with 20% fetal bovine serum and penicillin (100 μg ml^{-1})/streptomycin (250 ng ml^{-1})/amphotericin B at 33 °C in humid air containing 5% CO_2. After a series of passages, immortalized cells were obtained by frequent subculture for more than 4 months. Cell lines from different dishes were subcloned by limiting dilution. To induce cell differentiation, cells were treated with 3 μmol l^{-1} of 5-azacytidine for 24 hr. Subclones that included spontaneously beating cells were screened by microscopic observation (first screening), and cells surrounding spontaneous beating cells were subcloned with cloning syringes. Subcloned cells were maintained, exposed to 5-azacytidine again for 24 hr, and clones that showed spontaneous beating most frequently were screened (second screening). The clonal cell line thus obtained was named the CMG cell.

As a result of repeated rounds of limiting dilution, we succeeded in isolating 192 single clones, several of which differentiated into cardiomyocytes and showed spontaneous beating. The experiments were reproducible, but the percentage of cells that differentiated into cardiomyocyte differentiation was specific to each clones. Phase-contrast photography and/or immunostaining with anti-sarcomeric myosin antibodies were used to identify the morphological changes in the CMG cells. CMG cells showed a fibroblast-like morphology before 5-azacytidine treatment (0 week), and this phenotype was retained through repeated subculturing under non-stimulating conditions. After 5-azacytidine treatment, however, the morphology of the cells gradually changed (Figure 2). Approximately 10–30% of the CMG cells gradually increased in size at 1 week, and they formed ball-like appearance, or had lengthened in one direction to exhibit a stick-like morphology. Most of the other non-myocytes had an adipocyte-like appearance.

Regenerated cardiomyocytes display a fetal ventricular phenotype

Various cardiac contractile protein isoforms are differentially expressed in cardiomyocytes at different

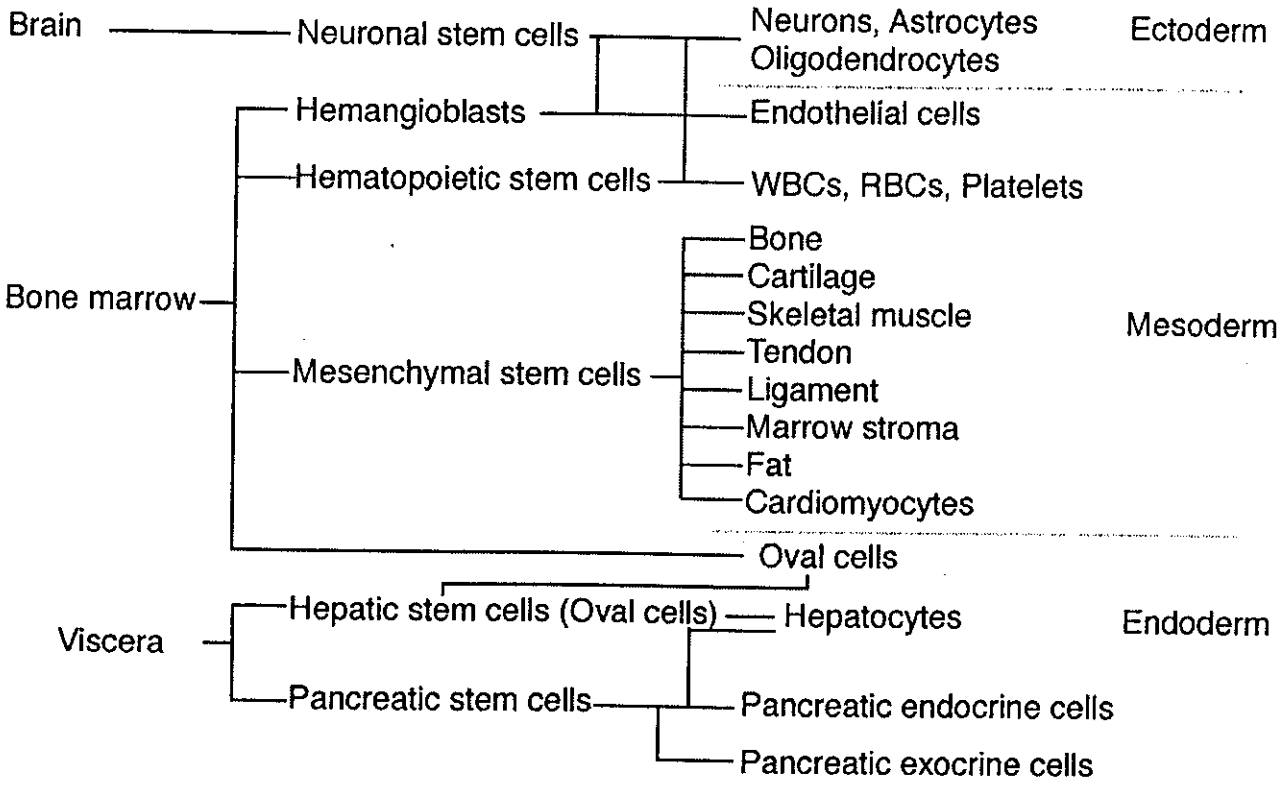

Figure 1. Classification of pluripotent stem cells in adult tissues. Bone marrow contains various kinds of stem cells. Mesenchymal stem cells may differentiate into various mesoderm-derived cells, such as osteoblasts, chondroblasts, adipocytes, skeletal muscle cells and possibly cardiomyocytes.

developmental stages and in different chambers. At around the time of birth there is a developmental switch in the ventricular muscle of small mammals from expression of β-myosin heavy chain (MHC), which is the predominant fetal form, to expression of α-MHC. There is also a developmental switch from expression of α-skeletal actin, which is the predominant fetal and neonatal form, to that of α-cardiac actin, the predominant adult form. We investigated the contractile protein isoforms of bone marrow-derived CMG cells to characterize their phenotype as cardiomyocytes. Table 1 summarizes the results. Fetal, neonatal, and adult ventricle and atrium were used as controls (Fukuda, 2001). Expression of both α- and *β-MHC* was detected in differentiated CMG cells by RT-PCR, but *β-MHC* expression was overwhelmingly greater than that of *α-MHC*. CMG cells expressed both *α-cardiac* and *α-skeletal actin*, but the *α-skeletal actin* gene was expressed at markedly higher levels than the *α-cardiac actin* gene. Interestingly, CMG cells expressed the *myosin light chain (MLC)-2v* gene, but not the *MLC-2a* gene. *MLC-2v* is specifically expressed in ventricular cells, while *MLC-2a* is specifically expressed in atrial cells. Skeletal muscle cells do not express either *α-MHC* or *MLC-2v*. These results indicated that differentiated CMG cells possess the specific phenotype of the fetal ventricular cardiomyocytes (Makino et al., 1999).

Developmental stage of undifferentiated and differentiated CMG cells

Various cardiac specific transcription factors have been cloned, and their genes are serially expressed in the developing heart during myogenesis and morphogenesis. Figure 3 shows the time course of the expression of cardiomyocyte-specific transcription factors in fetal developing heart and CMG cells. The genes coding Nkx2.5 (Linnets et al., 1993) (homeobox type transcription factor specifically expressed beginning in the early developing heart), GATA4 (Arceci et al., 1993) (GATA-motif-binding Zinc finger type transcription factor expressed beginning in the early stage developing heart), HAND1/2 (basic HLH type transcription factor expressed in the heart and autonomic

Table 1. Isoforms of the contractile proteins in differentiated CMG cells

Chamber	Atrium		Ventricle			CMG
Developmental stage	Fetus	Adult	Fetus	Neonate	Adult	
α-Actin	Skeletal	Cardiac	Skeletal > cardiac	Skeletal	Cardiac	Skeletal > cardiac
Myosin heavy chain	$\alpha > \beta$	α	$\beta > \alpha$	$\alpha > \beta$	α	$\beta > \alpha$
Myosin light chain	2a	2a	2v	2v	2v	2v

nervous system), and MEF2-B/C (Edmondson et al., 1994) (muscle enhancement factor: a MADS box family transcription factor expressed in the myocytes) were expressed in the early stage of heart development, and MEF2A and MEF2-D in the middle stage. The CMG cells already expressed *GATA4, TEF-1* (Chen et al., 1994) (transcription enhancement factor 2), *Nkx2.5, HAND*, and *MEF2-C* before exposure to 5-azacytidine, and they expressed *MEF2-A* and *MEF2-D* after exposure to 5-azacytidine. This pattern of gene expression in CMG cells was similar to that of developing cardiomyocytes *in vivo* (Makino et al., 1999), and indicated that the developmental stage of the undifferentiated CMG cells is close to that of cardiomyoblasts or the early stages of heart development. We estimated that the stage of differentiation of the CMG cells lies between the cardiomyocyte-progenitor stage and the differentiated cardiomyocyte stage.

Serial changes in action potential shape in CMG cells simulate those of fetal ventricular cardiomyocytes *in vivo*

CMG cells exhibit at least two types of distinguishable morphological action potentials: sinus-node-like potentials (Figure 4a) and ventricular myocyte-like potentials (Figure 4b) (Makino et al., 1999). The cardiomyocyte-like action potential recorded from these spontaneous beating cells is characterized by (1) a relatively long action potential duration or plateau, (2) a relatively shallow resting membrane potential, and (3) a pacemaker-like late diastolic slow depolarization. Peak-and-dome-like morphology was observed in ventricular-myocyte-like cells. Figure 4c shows the time course of the percentages of the sinus node-like and ventricular-myocyte-like action potentials. All action potentials recorded from CMG cells until 3 weeks were sinus-node-like action potential. The ventricular-myocyte-like action potentials were first recorded after 4 weeks, and their percentage gradually increased thereafter.

The observation of several distinct patterns of action potential in CMG cells may reflect different developmental stages. Yasui et al. studied action potentials and the occurrence of one of the pacemaker currents, I(f), by the whole-cell voltage and current-clamp technique at the stage when a regular heartbeat is first established (9.5 days post coitum) and at 1 day before birth (Yasui et al., 2001). They showed a prominent I(f) in mouse embryonic ventricles in the early stage, and that it decreased by 82% before birth in tandem with the loss of regular spontaneous activity by the ventricular cells. They concluded that the I(f) current of the sinus node type is present in early embryonic mouse ventricular cells. Loss of the I(f) current during the second half of embryonic development is associated with a tendency for the ventricle to lose pacemaker potency. Our findings in CMG cells may reflect the developmental changes in the action potentials that occur in embryonic ventricular cardiomyocytes.

Expression and function of α_1-adrenergic receptors in CMG cells

In the heart *in vivo*, α and β adrenergic receptors play a key role in modulating cardiac hypertrophy and cardiac function, such as heart rate, contractility, and conduction velocity. CMG cells expressed all the α_1 receptor subtypes (α_{1A}, α_{1B}, and α_{1D}) before 5-azacytidine exposure (Figure 5a) (Hakuno et al., 2002), and their expression in undifferentiated CMG cells may be explained by their ubiquitous or wide expression *in vivo* (Alonso-Llamazares et al., 1995). A low level of expression of α_{1A} was observed before 5-azacytidine exposure, and it increased markedly after exposure. Expression of α_{1B} was unaffected by 5-azacytidine. A high level of expression of α_{1D} was detected before 5-azacytidine exposure, but it decreased considerably after exposure. This tran-

Figure 2. Phase-contrast photographs of CMG cells before and after 5-azacytidine treatment. (Upper panel) CMG cells have a fibroblast-like morphology before 5-azacytidine exposure (0 week). (Middle panel) One week after treatment, some cells gradually increased in size, and developed a ball-like or stick-like appearance. (Lower panel) Two weeks after exposure, the ball-like or stick-like cells began spontaneous beating. Bars indicated 100 μm.

scriptional switch may be attributable to the CMG cells having acquired the cardiomyocyte phenotype. The ventricular cardiomyocytes *in vivo* mainly expressed α_{1A} and α_{1B}, and expressed a low level of α_{1D} receptor. The temporal changes in expression of α_1 adrenergic receptor subtypes in CMG cells are very

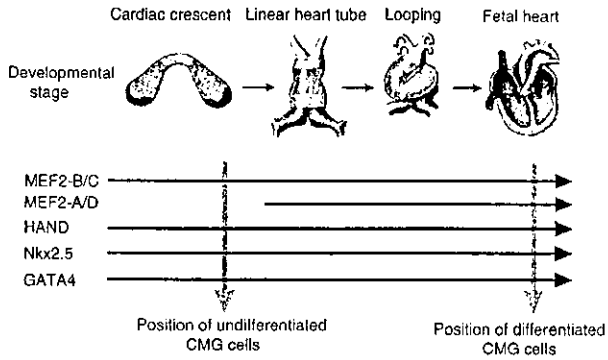

Figure 3. Expression of cardiac-specific transcription factors in the developing heart and in CMG cells. The horizontal arrows indicate the time course of the expression of cardiac-specific transcription factors in the developing fetal heart. The dotted vertical arrows indicate the expression of these factors in undifferentiated and differentiated CMG cells. CMG cells expressed MEF2-A and MEF2-D after 5-azacytidine exposure, when they acquired a cardiomyocyte phenotype.

similar to the postnatal changes observed in neonatal rat heart (Stewart et al., 1994; Rokosh et al., 1996).

ERK1/2 was activated by phenylephrine, an α_1 stimulant, within as little as 5 min, and the activation peaked at 10 min. The phenylephrine-induced phosphorylation was completely inhibited by prazosin (Figure 5b). Phenylephrine increased the cell area and perimeter of the CMG cardiomyocytes (Figure 5c). These findings indicated that CMG cells express functionally active α_1-adrenergic receptors (Hakuno et al., 2002).

Expression and function of β_1- and β_2-adrenergic receptors in CMG cells

The cardiomyocytes of the mammalian hearts express both β_1 and β_2-adrenergic receptors, the β_1 receptor being the predominant subtype (approximately 75–80% of total β receptors) (Rockman et al., 1997). CMG cells did not express β_1 and β_2 receptor transcripts before 5-azacytidine exposure, but RT-PCR showed expression of their mRNAs after 1 week (Figure 6a) (Hakuno et al., 2002). CMG cells expressed β_1 and β_2 mRNA after acquiring the cardiomyocyte phenotype. The temporal pattern of expression of these receptors differed from that of α_1.

Isoproterenol, a β stimulant, increased the cAMP content of CMG cells, and propranolol completely inhibited the isoproterenol-induced cAMP accumulation (Figures 6b and c). Isoproterenol was applied to the cells to determine whether it would increase the

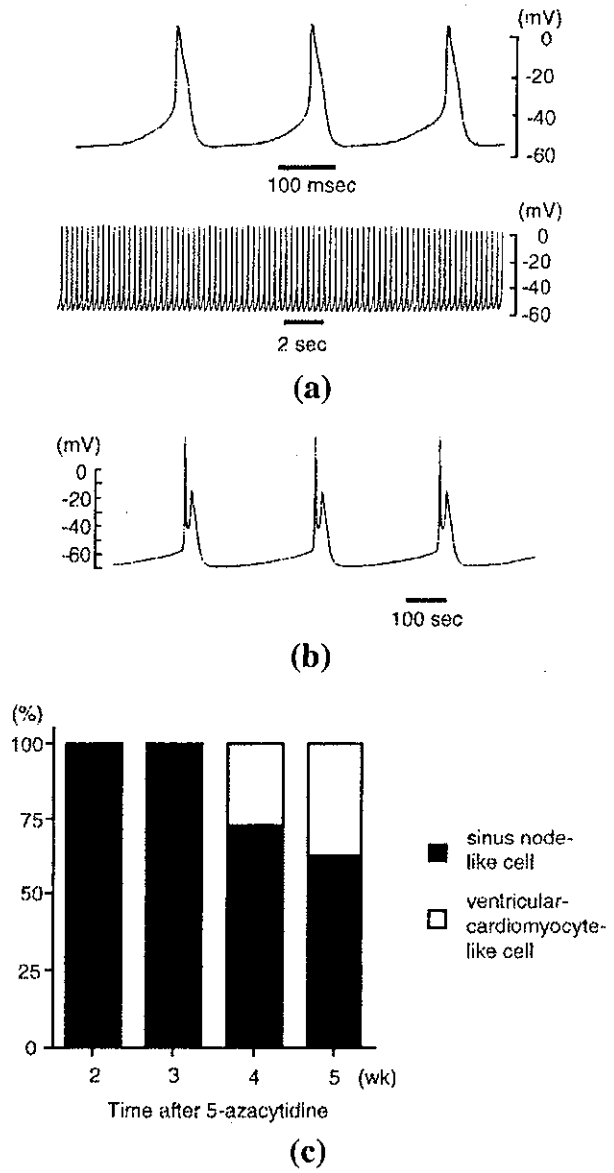

Figure 4. Representative tracing of the action potentials of CMG myotubes. (a, b) Action potential recordings from spontaneous-beating cells were obtained with a conventional microelectrode at day 28 after 5-azacytidine exposure. The action potentials were classified into two groups: (A) sinus-node-like action potentials and (B) ventricular-cardiomyocyte-like action potentials. (c) Percentages of CMG cells exhibiting sinus-node-like and ventricular-cardiomyocyte-like action potentials after 5-azacytidine exposure. A ventricular cardiomyocyte-like action potential was first recorded 4 weeks after 5-azacytidine exposure, and it rapidly became more predominant thereafter.

spontaneous beating rate (Table 2), and the results showed that it increased it significantly to 48% over the rate in the control cells (Hakuno et al., 2002). Preincubation with propranolol (non-sclective β blocker), CGP20712A (β_1-selective blocker) strongly reduced the isoproterenol-induced increase in beating rate, and preincubation with ICI118551 (β_2-selective blocker) only slightly decreased the beating rate. The increase in beating rate was similar to that of adult murine cardiomyocytes and ES cell-derived cardiomyocytes.

We also investigated the effect of isoproterenol on the contractile function of CMG cells and found that it increased cell motion distance, %shortening, and contractile velocity. The isoproterenol-induced increase in contractility was almost completely inhibited by both propranolol and CGP20712A. Collectively, these results indicated that the β_1 and β_2-adenergic receptors expressed in CMG cells are functional, and that the isoproterenol-induced increase in spontaneous beating rate and contractility is mainly mediated by β_1 receptors. The β_1 receptor was the predominant subtype that mediated changes in the beating rate in CMG cells, and the beating rate and the contractility were significantly increased by isoproterenol, and completely inhibited by propranolol and CGP20712A. β_1-Receptors played a critical role in mediating the isoproterenol-induced signaling in differentiated CMG cells. This expression pattern was consistent with that of cardiomyocytes *in vivo*.

CMG cells express muscarinic receptor mRNA after 5-azacytidine exposure

Heart rate, conduction velocity, and contractility were negatively regulated by the parasympathetic nervous system in cardiomyocytes, and muscarinic (cholinergic) receptors play an important role in mediating this function. To date, 5 subtypes (M_1-M_5) of muscarinic receptors have been cloned. The expression of the muscarinic receptors is tissue-specific, and cardiomyocytes mainly express M_2 receptors in the mouse and human (Sharma et al., 1997). The M_1 receptor subtype is also expressed in murine neonatal and adult cardiomyocytes. Figure 7a shows the temporal expression pattern of M_1 and M_2 receptor mRNA. Neither receptor was detected prior to 5-azacytidine exposure. CMG cells began to express these receptors when they acquired the cardiomyocyte phenotype.

M_1 receptors coupled to Gq/G_{11} and activated phospholipase C_β via $Gq\alpha$, leading to IP_3 production,

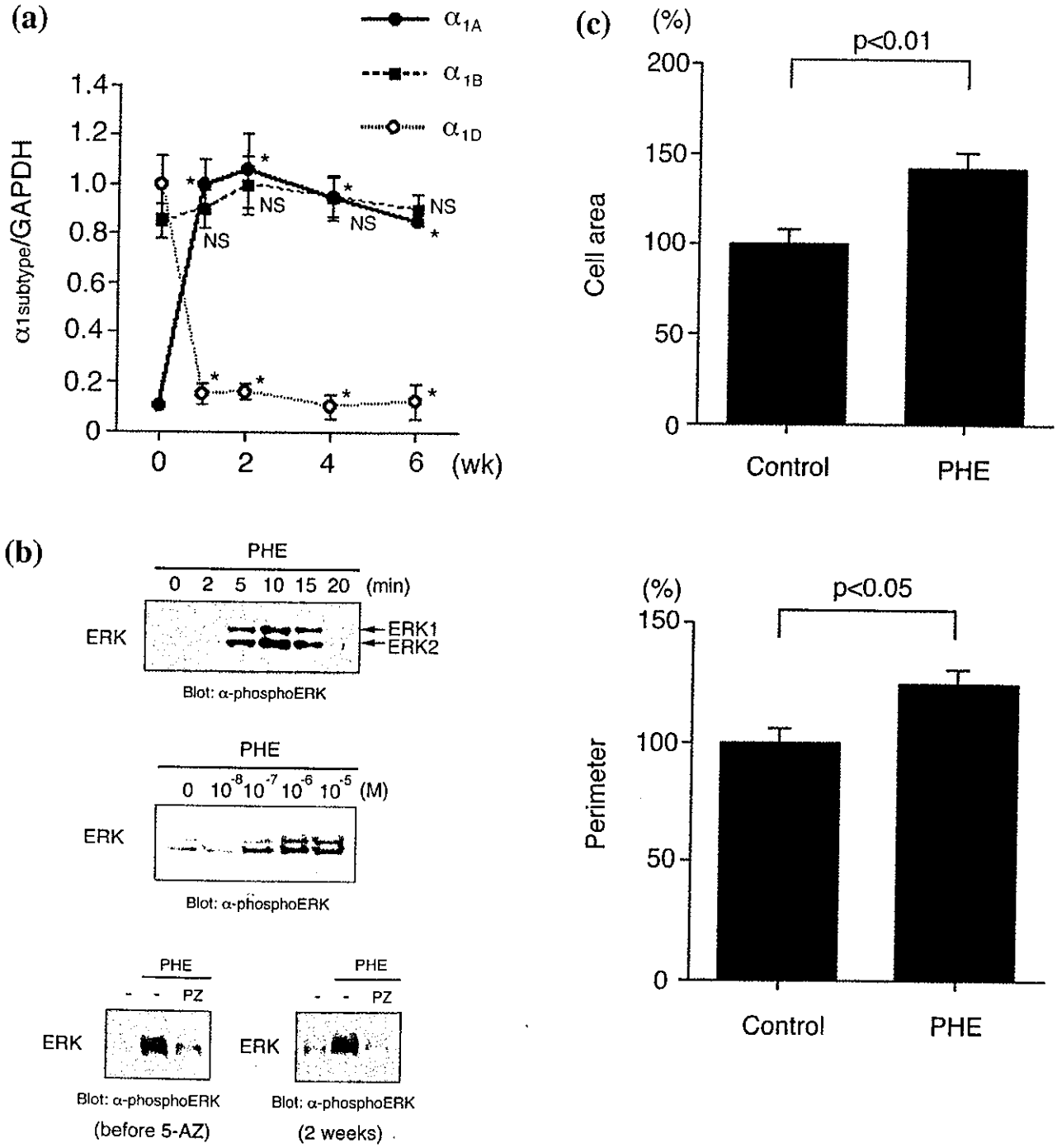

Figure 5. Expression and function of α_1-adrenergic receptor subtype in CMG cells. (a) Densitometric analysis was performed, and the ratio of the RT-PCR product of α_1 subtype (α_{1A}, α_{1B}, α_{1D}) receptors to that of GAPDH is shown. Data were obtained from 5 separate experiments and are shown in arbitrary units compared to the controls. Values are mean±SE. *: $p < 0.01$ vs. controls (before 5-azacytidine exposure). NS: not significant. (b) (Upper panel) Cells at 2 weeks after 5-azacytidine exposure were stimulated with phenylephrine (10^{-4} mol l^{-1}), and Western blot analysis was performed to detect phosphorylation of ERK1/2. (Middle panel) Cells were stimulated with phenylephrine (10^{-7}–10^{-5} mol l^{-1}) for 10 min, and phosphorylation of ERK was detected. (Lower panel) Prazosin (10^{-6} mol l^{-1}) was added to cells 20 min before stimulation with phenylephrine (10^{-6} mol l^{-1}). PHE: phenylephrine, PZ: prazosin. (c) Cells were serum depleted for 24 hr, stimulated with phenylephrine for 24 hr, and stained with anti-sarcomeric myosin antibody. Cell area and perimeter were quantitated with NIH Image software (n = 100) *: $p < 0.01$ vs. control.

Table 2. Isoproterenol increased the spontaneous beating rate and contractility of CMG cells, mainly via β_1 receptors

	Control	Isoproterenol (10^{-7} mol l^{-1})			
		Vehicle	Propranolol (10^{-7} mol l^{-1})	CGP20712A (10^{-7} mol l^{-1})	ICI118551 (10^{-7} mol l^{-1})
% Increase in beating rate	–	47.6±8.4*	10.0±1.9**	13.8±2.4**	37.6±1.9***
cell motion (μm)	5.0±0.3	6.8±0.7*	5.6±0.8***	5.3±0.6***	ND
% Shortening (%)	6.9±0.5	8.5±1.2*	7.2±0.8***	5.6±0.6***	ND
Contractile velocity (μm s^{-1})	71.1±5.2	100.9±11.0*	71.3±8.8***	70.6±6.6***	ND

CMG cells at 4 weeks after 5-azacytidine exposure were initially exposed to prazosin (10^{-6} mol l^{-1}) for 30 min to block α_1-adrenergic receptors. Cells were then preincubated for 20 min with vehicle (PBS), propranolol, CGP20712A, or ICI118551, and then stimulated with isoproterenol. The beating rate was counted 3 min after stimulation. Contractile parameters were analyzed 90 sec after stimulation. Each contractile parameter value was calculated as the mean of 3 randomly selected beats in one cell. PBS was added to the control. Values are means ± SE (n = 100, each). *: $p < 0.05$ vs. control, **: $p < 0.01$ vs. vehicle (isoproterenol only), ***: $p < 0.05$ vs. vehicle, ND: not determined.

and M_2 receptors coupled to $Gi/G_0/Gz$ and activated phospholipase C_β via $Gi\beta_\gamma$, leading to IP_3 production (Nakamura et al., 1995; Berstein et al., 1992). Carbachol, an acetylcholine homologue, increased the content of a second messenger, IP_3 (inositol triphosphate), in CMG cells (Figure 7b), and preincubation with atropine (non-selective muscarinic blocker) and AFDX116 (M_2-selective blocker) inhibited the carbachol-induced IP_3 production (Figure 7c). These findings indicated that muscarinic receptors can transduce their signals, and that M_2 receptors play a critical role in this carbachol-induced IP_3 production in CMG cells. This expression pattern is similar to that of cardiomyocytes *in vivo*.

Significance of expression of adrenergic and muscarinic receptors in CMG cells

Cardiomyocytes *in vivo* respond to stimulation by both sympathetic and parasympathetic nerves, and such stimulation alters the heart rate, conduction velocity, and contractility, enabling the cells to adapt to rapid changes in systemic oxygen demand. To date, and to our knowledge, ES cells and mesenchymal-stem-cell-derived CMG cells are the only possible candidates for regeneration of cardiomyocytes. We have already transplanted these cells into normal adult mouse hearts, and have observed that transplanted cells survived in recipient hearts for at least several weeks. Regenerated cardiomyocytes must express functional adrenergic and muscarinic receptors to be useful for transplantation, and although we did not investigate all signaling pathways and their functions. CMG cells are potential candidates for cardiomyocyte cell transplantation, because they possess such receptors.

Cell transplantation therapy for the treatment of heart failure

We have already transplanted CMG cells into normal adult mouse hearts, and observed that the transplanted cells could survive in the recipient heart for at least several months. Fibroblasts, smooth muscle cells, and skeletal muscle cells were the first cells used for transplantation into scar tissue secondary to experimental myocardial infarction in the heart *in vivo*. While transplantation of these cells into scar tissue might improve cardiac remodeling or diastolic function, it is unlikely to improve systolic function. Transplantation of cardiomyocytes, however, might rescue systolic function. The only potential sources of regenerated cardiomyocytes available to date are embryonic stem (ES) cells and mesenchymal stem cells. ES cells differentiate into cardiomyocytes *in vitro* and have both advantages and disadvantages for cardiomyocyte regeneration. Transplanted ES cells may form teratomas if some undifferentiated totipotent cells are still present, and

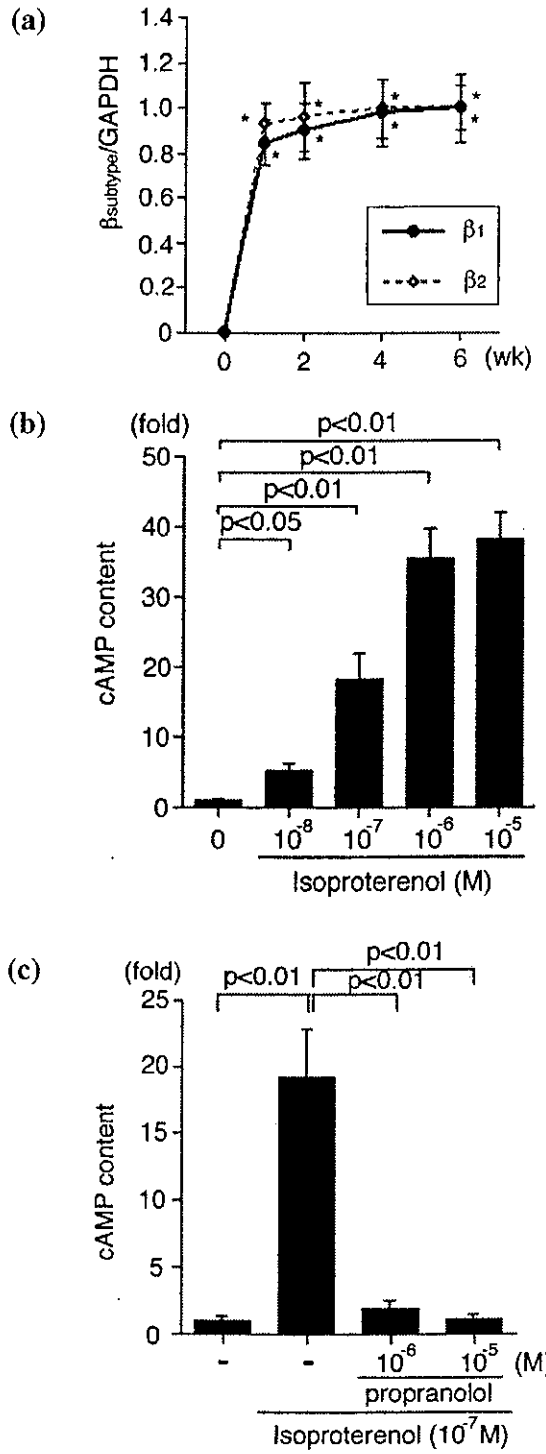

Figure 6. Expression and signal transduction of β_1- and β_2-adrenergic receptor subtype in CMG cells. (a) Densitometric analysis was performed, and the ratio of the RT-PCR product of β subtype (β_1 and β_2 receptors to that of GAPDH is shown. (b) Effect of isoproterenol on cAMP accumulation in CMG cells at 2 weeks after 5-azacytidine exposure. (c) Cells were preincubated with propranolol (10^{-6} or 10^{-5} mol l^{-1}) for 20 min and stimulated with isoproterenol (10^{-7} mol l^{-1}) for 10 min. Data were obtained from 5 separate experiments and are shown as arbitrary units compared with the controls. *: $p < 0.01$, **: $p < 0.05$ vs. controls.

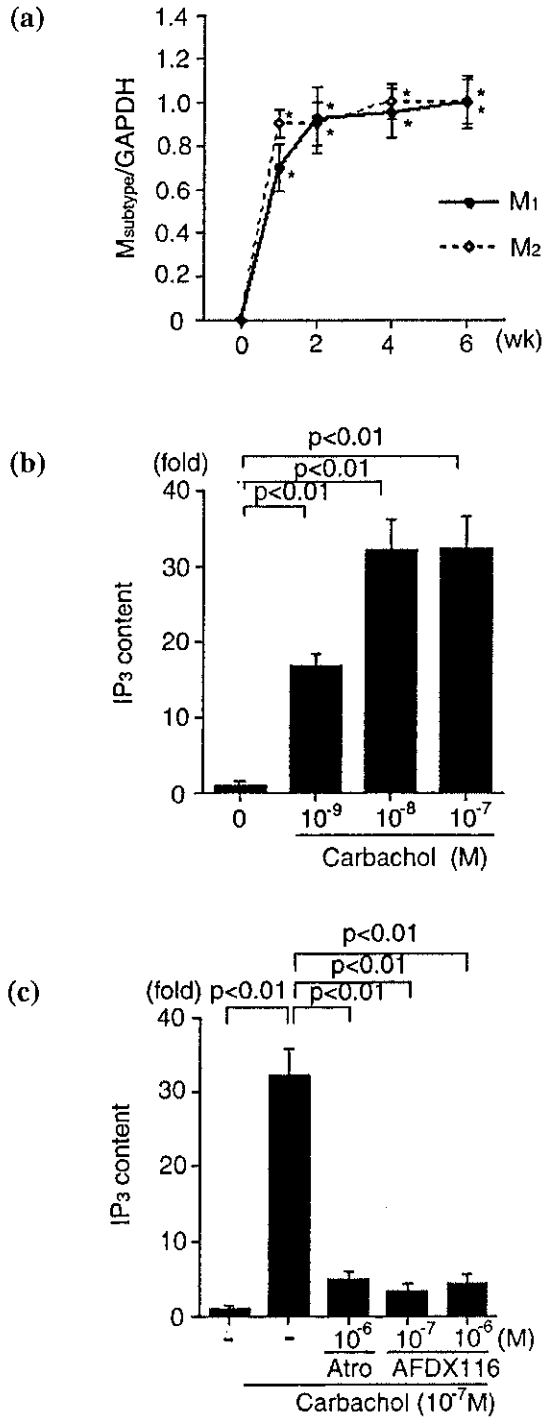

Figure 7. Expression and function of M_1- and M_2-muscarinic receptors in CMG cells. (a) The ratio of the RT-PCR product of muscarinic subtype to that of GAPDH is shown. Data were obtained from 5 separate experiments and are shown as arbitrary units over controls. *: $p < 0.01$ vs. controls. (b) Effect of carbachol on IP_3 production in CMG cells at 2 weeks after 5-azacytidine exposure. (c) Effect of atropine (10^{-6} mol l^{-1}) and AFDX116 (10^{-7} or 10^{-6} mol l^{-1}) on carbachol-induced IP_3 production. Data were obtained from 5 separate experiments and are shown as arbitrary units compared with the controls. *: $p < 0.01$ vs. controls. Atro: atropin.

recipients must take immunosuppressants, because ES cells are allogeneic. By contrast, since mesenchymal stem cells do not carry any inherent risks of tumor formation and are syngeneic, it is reasonable to use autologous mesenchymal stem cell to treat heart disease. Nevertheless, there is a need to improve both the current methods for identification and culture of mesenchymal stem cells, and for induction of CMG cell differentiation, which are still inefficient and slow. Identification of specific growth factors, cytokines, or extracellular matrix factors that regulate cardiomyocyte differentiation may help to accelerate this process faster and make it more efficient.

In vivo evidence that marrow cells can generate functional cardiac tissues

Recent studies have revealed that bone-marrow-derived cells differentiate into various types of cells *in vivo*. Shimizu et al. reported that smooth-muscle-like cells (SMCs) in graft-vs-host arterial lesions could arise from circulating bone-marrow-derived precursors. They used murine aortic transplants to formally identify the source of SMCs in lesions in grafted arteries (Shimizu et al., 2001). Allografts in beta-galactosidase transgenic recipients showed that intimal SMCs arose almost exclusively from host cells, and bone-marrow transplantation of beta-galactosidase-expressing cells into aortic allograft recipients demonstrated that the intimal cells included those of marrow origin.

Kocher et al. (2001) showed that bone marrow from adult humans contains endothelial precursors with phenotypic and functional characteristics of embryonic hemangioblasts and that they can be used to directly induce new blood vessel formation in the infarct-bed (vasculogenesis) and proliferation of preexisting vasculature (angiogenesis) after experimental myocardial infarction. The neoangiogenesis resulted in decreased apoptosis of hypertrophied myocytes in the peri-infarct region, long-term salvage and survival of viable myocardium, reduction in collagen deposition, and sustained improvement in cardiac function.

We also observed that transplanted bone marrow cells differentiated into cardiomyocytes in the recipient heart *in vivo* (unpublished observation). These findings provided direct evidence that bone marrow cells can regenerate various types of cells in cardiac tissue. We expect cardiac tissues damaged by myocardial infarction or other diseases to be repaired by bone-marrow-derived stem cells in the near future, and the precise mechanism should be investigated to achieve this goal.

References

Alonso-Llamazares A, Zamanillo D, Casanova E, Ovalle S, Calvo P & Chinchetru MA (1995) Molecular cloning of alpha 1d-adrenergic receptor and tissue distribution of three alpha 1-adrenergic receptor subtypes in mouse. J Neurochem 65: 2387–2392.

Arceci RJ, King AA, Simon MC, Orkin SH & Wilson DB (1993) Mouse GATA-4: A retinoic acid-inducible GATA-binding transcription factor expressed in endodermally derived tissues and heart. Mol Cell Biol 13: 2235–2246.

Ashton BA, Allen TD, Howlett CR, Eaglesom CC, Hattori A & Owen M (1980) Formation of bone and cartilage by marrow stromal cells in diffusion chambers *in vivo*. Clin Orthop 151: 294–307.

Berstein G, Blank JL, Smrcka AV, Higashijima T, Sternweis PC, Exton JH & Ross EM (1992) Reconstitution of agonist-stimulated phosphatidylinositol 4,5-bisphosphate hydrolysis using purified m1 muscarinic receptor, Gq/11, and phospholipase C-beta 1. J Biol Chem 267: 8081–8088.

Chen Z, Friedrich GA & Soriano P (1994) Transcriptional enhancer factor 1 disruption by a retroviral gene trap leads to heart defects and embryonic lethality in mice. Genes Dev 8: 2293–2301.

Delcarpio JB & Claycomb WC (1997) Cardiomyocyte transfer into the mammalian heart. Cell-to-cell interactions *in vivo* and *in vitro*. Ann NY Acad Sci 52: 267–285.

Edmondson DG, Lyons GE, Martin JF & Olson EN (1994) Mef2 gene expression marks the cardiac and skeletal muscle lineages during mouse embryogenesis. Development 120: 1251–1263.

Ferrari G, Angelis GC, Colleta M, Paolucci E, Stornaiolo A, Cossu G & Mavilio F (1998) Muscle regeneration by bone marrow-derived myogenic progenitors. Science 279: 1528–1530.

Friedenstein AJ, Chailakhyan R & Gerasimov UV (1987) Bone marrow osteogenic stem cells: *In vitro* cultivation and transplantation in diffusion chambers. Cell Tissue Kinet 20: 263–272.

Fukuda K (2001) Development of regenerative cardiomyocytes from mesenchymal stem cells for cardiovascular tissue engineering. Artif Organs 25: 183–193.

Hakuno D, Fukuda K, Makino S, Konishi F, Tomitra Y, Manabe T, Suzuki Y, Hisaka Y, Umezawa A & Ogawa S (2002) Bone marrow-derived cardiomyocytes (CMG cell) expressed functionally active adrenergic and muscarinic receptors. Circulation 105: 380–386.

Kocher AA, Schuster MD, Szabolcs MJ, Takuma S, Burkhoff D, Wang J, Homma S, Edwards NM & Itescu S (2001) Neovascularization of ischemic myocardium by human bone-marrow-derived angioblasts prevents cardiomyocyte apoptosis, reduces remodeling and improves cardiac function. Nat Med 7: 430–436.

Linnets TJ, Parsons LM, Harley L, Lyons I & Harvey RP (1993) Nkx-2.5: A novel murine homeboy gene expressed in early heart progenitor cells and their myogenic descendants. Development 119: 419–431.

Makino S, Fukuda K, Miyoshi S, Konishi F, Kodama H, Pan J, Sano M, Takahashi T, Hori S, Abe H, Hata J, Umezawa A & Ogawa S, (1999) Cardiomyocytes can be generated from marrow stromal cells *in vitro*. J Clin Invest 103: 697–705.

Nakamura F, Kato M, Kameyama K, Nukada T, Haga T, Kato H, Takenawa T & Kikkawa U (1995) Characterization of Gq family G proteins G_{L1} alpha (G_{14} alpha), G_{L2} alpha (G_{11} alpha), and Gq alpha expressed in the baculovirus-insect cell system. J Biol Chem 270: 6246–6253.

Prockop DJ (1997) Marrow stromal cells as stem cells for nonhematopoietic tissues. Science 276: 71–74.

Rickard DJ, Sullivan TA, Shenker BJ, Leboy PS & Kazhdan I (1994) Induction of rapid osteoblast differentiation in rat bone marrow stromal cell cultures by dexamethasone and BMP-2. Dev Biol 161: 218–228.

Rockman HA, Koch WJ & Lefkowitz RJ (1997) Cardiac function in genetically engineered mice with altered adrenergic receptor signaling. Am J Physiol 272: H1553–H1559.

Rokosh DG, Stewart AF, Chang KC, Bailey BA, Karliner JS, Camacho SA, Long CS & Simpson PC (1996) Alpha1-adrenergic receptor subtype mRNAs are differentially regulated by alpha1-adrenergic and other hypertrophic stimuli in cardiac myocytes in culture and *in vivo*. Repression of alpha1B and alpha1D but induction of alpha1C. J Biol Chem 271: 5839–5843.

Roy NS, Wang S, Jiang L, Kang J, Benraiss A, Harrison-Restelli C, Fraser RA, Couldwell WT, Kawaguchi A, Okano H, Nedergaard M & Goldman SA (2000) In vitro neurogenesis by progenitor cells isolated from the adult human hippocampus. Nat Med 6: 271–277.

Sharma VK, Colecraft HM, Rubin LE, Sheu SS (1997) Does mammalian heart contain only the M_2 muscarinic receptor subtype? Life Sci 60: 1023–1029.

Shimizu K, Sugiyama S, Aikawa M, Fukumoto Y, Rabkin E, Libby P & Mitchell RN (2001) Host bone-marrow cells are a source of donor intimal smooth-muscle-like cells in murine aortic transplant arteriopathy. Nat Med 7: 738–741.

Soonpaa MH, Koh GY, Klug MG & Field LJ (1997) Formation of nascent intercalated disks between grafted fetal cardiomyocytes and host myocardium. Science 264: 98–101.

Stewart AF, Rokosh DG, Bailey BA, Karns LR, Chang KC, Long CS, Kariya K & Simpson PC (1994) Cloning of the rat alpha 1C-adrenergic receptor from cardiac myocytes. alpha 1C, alpha 1B, and alpha 1D mRNAs are present in cardiac myocytes but not in cardiac fibroblasts. Circ Res 75: 796–802.

Wobus AM, Wallukat G & Hescheler J (1991) Pluripotent mouse embryonic stem cells are able to differentiate into cardiomyocytes expressing chronotropic responses to adrenergic and cholinergic agents and Ca^{2+} channel blockers. Differentiation 48: 173–182.

Wobus AM, Kleppisch T, Maltsev V & Hescheler J (1994) Cardiomyocyte-like cells differentiated *in vitro* from embryonic carcinoma cells P19 are characterized by functional expression of adrenoceptors and Ca^{2+} channels. In Vitro Cell Dev Biol Anim 30: 425–434.

Yasui K, Liu W, Opthof T, Kada K, Lee JK, Kamiya K & Kodama I (2001) I(f) current and spontaneous activity in mouse embryonic ventricular myocytes. Circ Res 88: 536–542.

Int. J. Dev. Biol. 47: 405-410 (2003)

Original Article

Amphibian *in vitro* heart induction: a simple and reliable model for the study of vertebrate cardiac development

TAKASHI ARIIZUMI[1], MASAYOSHI KINOSHITA[2], CHIKA YOKOTA[3], KAZUHIRO TAKANO[3], KEIICHI FUKUDA[2], NOBUO MORIYAMA[1], GEORGE M. MALACINSKI[4] and MAKOTO ASASHIMA*[,3]

[1]*Department of Experimental Nursing, Faculty of Nursing, Fukuoka Prefectural University, Fukuoka, Japan,* [2]*Cardiopulmonary Division, Department of Internal Medicine, Institute for Advanced Cardiac Therapeutics, Keio University School of Medicine, Tokyo, Japan,* [3]*Department of Life Sciences (Biology), Graduate School of Arts and Sciences, SORST, Japan Science and Technology Corporation (JST), The University of Tokyo, Tokyo, Japan and* [4]*Department of Biology, Indiana University, Bloomington, Indiana, USA*

ABSTRACT Amphibian embryos are an excellent model system for analyzing the mechanisms of vertebrate cardiogenesis. Studies of heart development in *Xenopus* have, for example, revealed that the inductive interaction of the heart primordia with the adjacent underlying endoderm and dorsal lip starts at the early stages of gastrulation. However, the molecular basis of those early inductive events and the genes expressed during the early phases of heart differentiation remain largely unknown. Amphibian blastula embryos contain pluripotent cells in their ectodermal region, called the "animal cap," which fortunately can be exploited for understanding a variety of organogenesis processes. Despite an enormous potential for analysis, the use of this system in cardiogenesis research has languished due to a lack of information concerning appropriate culture methods. Herein we report conditions for generating an *in vitro* heart induction system and present evidence from two types of *in vivo* transplantations, that the cultured heart rudiment can develop and function in the adult organism. It is expected that the fundamental principles established in this model system will provide a versatile research platform for a variety of organ engineering projects, including modifying *in vitro* organ growth with exogenous components (e.g. various growth factors) and developing methods for preparing tissue for transplantation.

KEY WORDS: *activin, animal cap, cardiogenesis, organ engineering, transplantation*

Introduction

Previous attempts at exploiting the convenience of the amphibian embryonic system as a model for vertebrate heart development have yielded mixed results.

Reproducibility as well as percentage yield for organ cultures has varied from experiment to experiment. As well, morphological and histological criteria have often been employed as the main assessment criteria for differentiation. Finally, accurate measurements of functional capacity of developed organ cultures have not always been performed.

Nevertheless, progress is being achieved on many aspects of amphibian heart organ culture including the identification of potential regulatory circuits which govern signaling between inducing and responding tissues. In *Xenopus*, for example, a role for the Wnt antagonists DKK-1 and Cresent has been proposed (reviewed by Schneider and Mercol, 2001). In this report we further refine the *Xenopus* organ culture system for cardiac differentiation, and provide protocols and results which enhance the suitability of this model system. A key step in the protocol, a dissociation/reaggregation procedure, is outlined and *in vivo* ectopic transplantation exercises are conducted to unambiguously assess the functional capacity of cytodifferentiated cultures.

Results

As the first phase of this study, we developed a completely new protocol for preparing a reliable *in vitro* heart induction system using *Xenopus* blastula animal caps (Fig. 1A). Dissected animal caps were dissociated into individual cells by treatment with calcium-free saline. The dissociated cells were then reaggregated by placing them in a standard saline solution containing calcium. During the latter process, cells were exposed to activin (10-1,000 ng/ml), a peptide growth factor (Asashima *et al.*, 1990) for 1-72 h. In the absence of

***Address correspondence to:** Dr. Makoto Asashima. Department of Life Sciences (Biology), Graduate School of Arts and Sciences, The University of Tokyo, 3-8-1 Komaba, Meguro-ku, Tokyo 153-8902, Japan. Fax: +81-3-5454-6998. e-mail: asashi@bio.c.u-tokyo.ac.jp

Electronic Supplementary Material for this paper, consisting of four "QuickTime" movies is avaliable at the following address: http://www.ijdb.ehu.es/abstract.0306/esm1.htm

0214-6282/2003/$25.00

Printed in Spain
www.ijdb.ehu.es

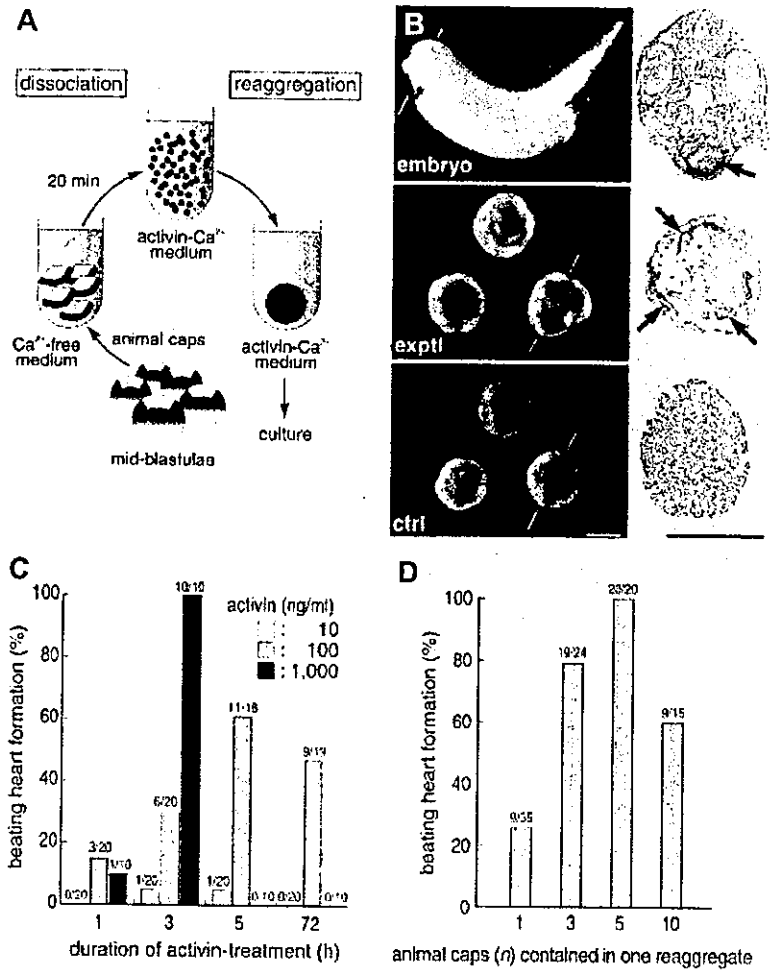

Fig. 1. *In vitro* heart induction system using embryonic pluripotent cells. (A) *The dissociation/reaggregation protocol for* in vitro *heart induction. The cell adhesion of mid-blastula animal caps were loosened in Ca^{2+}-free medium. Dissociated (by gentle pipetting) cells began to form a spherical reaggregate in the medium containing Ca^{2+} and an appropriate concentration of activin.* **(B)** Xenopus cardiac troponin I *(XTnIc), a marker gene for myocardial differentiation, expressed specifically in myocardium of a normal 3-day-old embryo (upper). The dissociated animal cap cells formed spherical reaggregates, regardless of whether they had been treated with activin. However, untreated reaggregates showed negative staining of the* XTnIc *signal after they were cultured for 3 days (lower).* XTnIc *signals were detected only in activin-treated reaggregates (middle). Note the* XTnIc *signals (arrows) at the tubular hearts on the transverse sections of the normal embryo and the activin-treated reaggregate. Scale bar, 0.5 mm.* **(C)** *Activin frequently induced beating hearts at concentrations higher than 100 ng/ml. The frequency of beating-heart formation reached 100% when the animal cap cells were treated with 1,000 ng/ml activin for 3 h. Each reaggregate was comprised of 10 animal caps (approx. 2,000 cells).* **(D)** *The number of cells contained in a reaggregate also affected heart formation. The dissociated cells were treated with 100 ng/ml activin for 5 h in this experiment. The frequency of heart formation reached 100% when 5 animal caps (approx. 1,000 cells) were contained in a reaggregate. The number on the top of each column refers to the number of reaggregates with beating hearts per the total number of reaggregates.*

activin, no tissue differentiation other than atypical epidermis was found in the reaggregates after 3 days of culture. Conversely, activin treatment (e.g., 100 ng/ml, for 5 h) caused the formation of beating tissue inside the thin epidermal vesicle. These tissues often showed tubular or globular morphology and contracted regularly (Supplementary Movie 1). Whole-mount *in situ* hybridization of the *XTnIc* (*Xenopus cardiac troponin I*) gene that is ordinarily expressed specifically in the mycardium of the heart (Drysdale *et al.*, 1994) revealed that these beating tissues were undoubtedly heart-like (Fig. 1B). These *in vitro*-induced hearts kept beating rhythmically for more than 2 weeks without a change in the culture medium. The heartbeat rate of the induced cultures depended on the ambient temperature, which is also true of the heartbeat rate in intact, normal embryos. For example, the heartbeat rates of the 1-week-cultured hearts increased about fivefold at 24°C (76 ± 5 bpm, n=5) compared to the rates at 5°C (16 ± 5 bpm). Electron microscopy revealed that the induced hearts exhibited a clear cytodifferentiation pattern typical of normal embryonic hearts. Myocardial cells with well-organized myofibrils joined at a junctional zone called the intercalated disc (data not shown).

Previous studies indicated that activin's inducing effects on animal caps depend on both concentration and treatment time (Asashima *et al.*, 2000; Ariizumi and Asashima, 2001; Ariizumi *et al.*, 1991; Asashima *et al.*, 1999). We therefore determined the optimal conditions for activin action on *in vitro* heart induction. The effect of treatment time at three activin concentrations on reaggregates comprised of cells (approx. 2,000) from 10 animal caps was examined (Fig. 1C). Three hours at 1,000 ng/ml yielded beating hearts in all (100%) of the cultures, while treatment with 100 ng/ml for 5 h yielded beating hearts in 60% of the cultures. The number of cells contained in a reaggregate also affected the success rate for beating hearts (Fig. 1D). Reaggregates of 5 animal caps (approx. 1,000 cells) yielded complete heart induction by treatment with 100 ng/ml of activin for 5 h. These data validate our procedure as a reliable method for using multipotent amphibian cells in the study of heart induction *in vitro*.

Next, we performed RT-PCR analyses using several marker genes to evaluate the significance of the "dissociation/reaggregation" step to this *in vitro* heart induction system. Following treatment with activin (100 ng/ml), striking differences in the early gene expression pattern were recognized between the undissociated animal caps and reaggregates (Fig. 2A). The expression levels of an early neural marker, *XSox2*, and mesodermal markers (*Xbra*, *XWnt-11*, and *XNot*) were constantly maintained in the intact animal caps, whereas those of *XGATA-4* (an early marker for both heart and anterior endoderm [Jiang and Evans, 1996]) and endodermal markers (*XHex* and *XSox17β*) sharply decreased starting at 9 h after the initial treatment with activin. Conversely, early expression of

neural and mesodermal markers (up to 5h) and prolonged expression of *XGATA-4* and *Xhex* were observed when the animal caps were subjected to the dissociation/reaggregation step. An early heart-field marker *XNkx2.5* (Tonissen *et al.*, 1994) gradually increased its expression level starting at 5 h after the beginning of activin treatment.

The differences in the gene expression patterns became clearer when those animal cap explants were cultured for 3 days (Fig. 2B). Following treatment with activin, the undissociated animal caps still expressed neural and mesodermal markers. Expression of heart-specific marker genes was entirely absent in those tissue samples. In contrast, animal cap tissue that was first dissociated, then treated with activin, and finally reaggregated expressed neither neural nor mesodermal markers. Instead, it expressed heart field markers *XNkx2.5*, *XGATA-4*, and *XTbx5* (Horb and Thomsen, 1999) or cardiomyocyte markers *XMHCα* (Logan and Mohun, 1993), *XTnIc*, and *XANF* (*Xenopus* atrial natriuretic factor [Small and Krieg, 2000]). The expression of *endodermin*, a pan-endodermal marker gene, was induced in the animal cap cells that received activin treatment alone, irrespective of dissociation/reaggregation. These results clearly indicate that the dissociation/reaggregation protocol is the key step for achieving heart differentiation in activin-induced animal cap tissue.

In order to determine whether these *in vitro*-induced hearts are functionally active, two types of transplantation experiments (Fig. 3A), based on protocols devised by Grunz (1999), were performed. In one type of manipulation, replacement transplantation, a fragment of a reaggregate of activin-treated animal cap cells was used as a donor. Donor reaggregates were precultured in saline for 1 day prior to transplantation into late neurula recipient embryos. Removal of the heart primordia from neurulae (control: no donor transplant tissue) resulted in development of edema and death within several days or at most 2 weeks. When an *in vitro*-induced heart rudiment was transplanted to the site from which the original heart primordium had been removed, 74% (217 of 294) of experimental embryos developed normally for 5 days (Fig. 3B). The donor heart began to contract 1 day after transplantation, which corresponded to the same time at which the normal embryonic heart in untreated normal embryos begins beating. Cell-lineage analyses using fluorescent dyes revealed that the donor hearts contained a few blood cells derived from the recipient (data not shown). Almost all embryos (210 of 217) could not suppress the onset of edema thereafter and died within 2 weeks. One of the 7 remaining embryos survived for 76 days after the transplantation and reached developmental stage 56 (Nieuwkoop and Faber, 1956). However, it did not succeed in metamorphosing into adult.

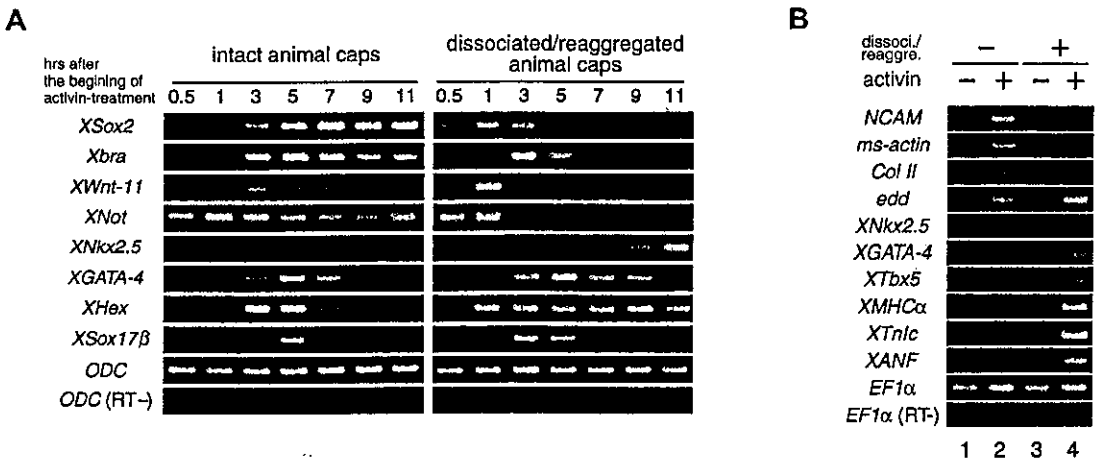

Fig. 2. Gene expression patterns of the *in vitro*-induced heart rudiments. (A) *Comparison of early gene expression patterns between the intact (undissociated) and dissociated/reaggregated animal caps after activin treatment (100 ng/ml). The left-hand column indicates the time course of gene expressions in the intact but activin-induced animal caps. Neural and mesoderm differentiation markers (*XSox2 *and* Xbra/XWnt-11/XNot, *respectively) expressed constantly when the animal caps were treated with activin for more than 3 h. Conversely, the expressions of* XGATA-4 *(a marker for both heart and anterior endoderm),* XHex *(for anterior endoderm), and* XSox17β *(for pan-endoderm) disappeared by treating with activin for more than 9 h. Note that* XNkx2.5, *an early heart-field marker, was never detected in these samples. The right-hand column shows the profile of gene expressions in the animal caps after the combined activin and dissociation/reaggregation treatments. In contrast to the profile in the left-hand column, the expressions of the neural and mesoderm markers were faded out by exposure to activin for more than 5 h. The expressions of* XGATA-4 *and* XHex *were maintained for at least 9 h after the beginning of activin treatment. Note that* XNkx2.5 *was initially detected at 5 h after the beginning of activin treatment and gradually increased its expression level.* ODC, *loading control; (RT-), negative control lacking reverse transcriptase.* **(B)** *Gene expression patterns in the intact or reaggregated animal caps cultured for 3 days. Non-activin-induced cells expressed none of the markers even after they were subjected to the dissociation/reaggregation protocol (lanes 1 and 3). Activin treatment (100 ng/ml, 5 h) induced the expression of the pan-neural (*NCAM*), muscle (*ms-actin*), and notochord (*Col II*) markers in intact animal caps cultured for 3 days (lane 2). No heart-specific marker was detected in these samples. By contrast, the reaggregates consisting of activin-induced cells exclusively expressed all of the heart-differentiation markers, such as* XNkx2.5, XGATA-4, XTbx5, XMHCα, XTnIc, *and* XANF *(lane 4). The expression of* endodermin *(*edd*), a pan-endoderm marker, was induced by activin treatment, irrespective of dissociation/reaggregation (lanes 2 and 4).* EF1α, *loading control; (RT-), negative control lacking reverse transcriptase.*

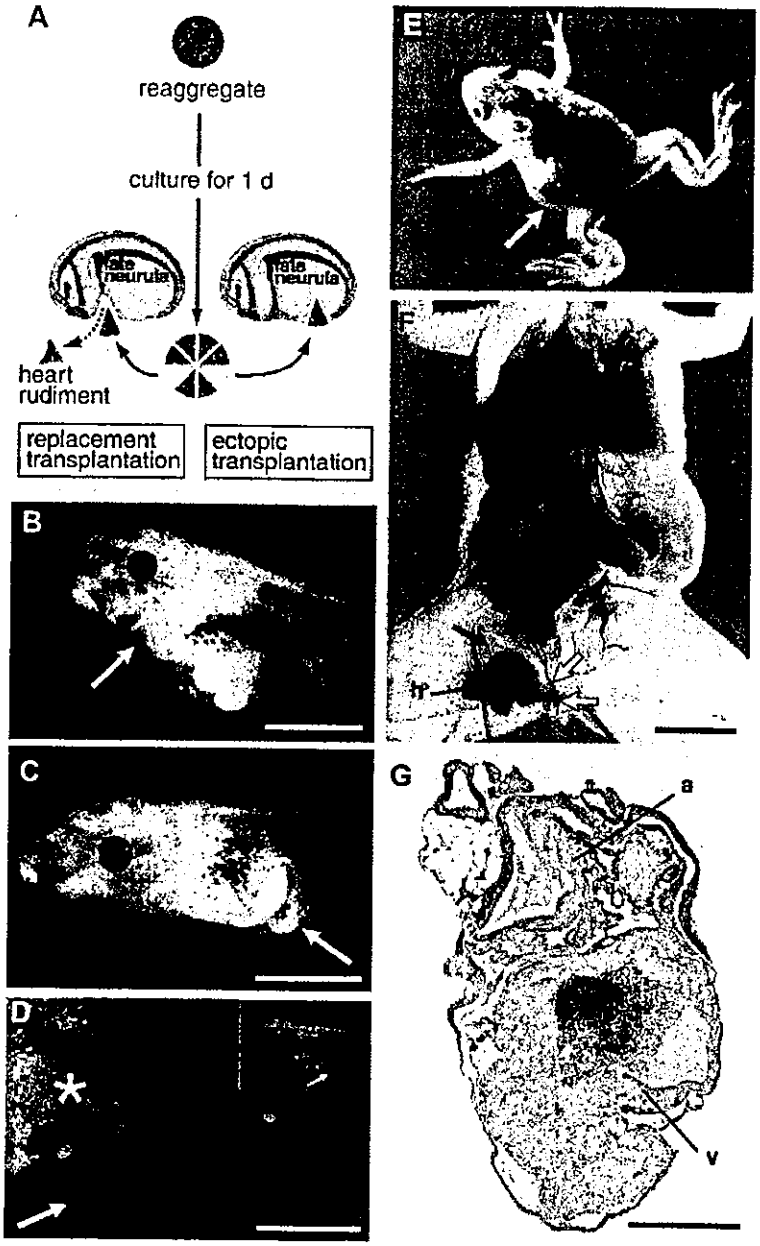

Fig. 3. *In vivo* transplantation of the *in vitro*-induced heart rudiments. (A) *Two types of* in vivo *heart transplantations. Following preculture for 1 day, a fragment of reaggregate was transplanted as donor tissue into late neurulae. The original heart rudiment of the host embryo was replaced with a donor heart rudiment in replacement transplantation, while a donor fragment was inserted into a slit made in the host's abdomen in ectopic transplantation.* **(B)** *Embryos that received a replacement transplantation of an* in vitro*-induced heart developed normally for 5 days. The substitute heart (arrow) was beating regularly and contained a small amount of host blood cells in its interior. Scale bar, 1 mm.* **(C)** *Embryos which received an ectopic transplantation developed normally without edema formation. The ectopic heart (arrow) contained a large number of red blood cells derived from the host embryo. Scale bar, 1 mm.* **(D)** *Cell-lineage analysis of an ectopic transplantation revealed that the ectopic heart (red, arrow) contained blood cells (green, asterisk) of the host. The external view of the embryo is shown in the upper right. Scale bar, 0.1 mm.* **(E)** *A young frog which was ectopically transplanted with an* in vitro*-induced heart rudiment at the neurula stage. In vitro-induced hearts remained in the recipients' left abdomen even after they had metamorphosed into frogs. An ectopic heart (arrow) filled with red blood cells can easily be seen through the thin skin.* **(F)** *Example of internal anatomy of an 1-year-old frog with a well-developed ectopic heart. The ectopic heart (h) adjacent to the host's intestine was incorporated into the host's vascular system. The blood from the host's mesenteric artery (black arrows) was flowing into the host's anterior abdominal vein (white arrows) via the ectopic heart. Scale bar, 5 mm.* **(G)** *Histological section of an ectopic heart. The heart can be divided into two chambers, a thin atrium (a) and a thick ventricle (v), based on the thickness of myocardium. r, red blood cells; scale bar, 0.5 mm.*

These observations are most likely explained by the incomplete connection of the donor heart with the host's main blood vascular and pronephric systems (Chan *et al.*, 1999).

In the other type of manipulation, ectopic transplantation, an activin-induced animal cap reaggregate was transplanted into a slit made in the posterior abdomen of a recipient neurula embryo. Fifty percent (276 of 547) of the recipients developed normally through morphogenesis except for exhibiting an ectopic beating heart (Fig. 3C). Both host and ectopic hearts began to contract at 1 day after transplantation. Large numbers of red blood cells were easily recognized through the thin envelope of the ectopic heart (Supplementary Movie 2). As in the replacement transplantations, cell lineage analyses revealed that these blood cells were derived from the host embryo (Fig. 3D). Further, we have succeeded in raising through metamorphosis 29% (80 of 276) of these ectopic transplants into adults. In one remarkable case, the donor heart hypertrophied at the abdomen of the host frog and thus its beating could be externally monitored (Fig. 3E and Supplementary Movie 3).

Additional analyses were carried out by dissecting 33 of 80 recipients (aged approximately 1 year) at random. A well-developed ectopic heart integrated with the host's blood vascular system was readily observed in all samples (Supplementary Movie 4). The ectopic heart, located adjacent to the host's intestine, was beating at nearly the same rate as the host's heart. Clamping the host's anterior abdominal vein caused the expansion of the ectopic heart, revealing blood circulation between the ectopic heart and the host's blood vascular system. A detailed analysis of a video recording of the internal anatomy of one such specimen indicted that blood was circulating from a branch of the host's mesenteric arteries to the ectopic heart (Fig. 3F). The blood from that ectopic heart flowed into the host's anterior abdominal vein. Examination of histological sections revealed that the ectopic heart could be divided into at least two chambers (atrium and ventricle) based on the thickness of the myocardium (Fig. 3G).

Discussion

A variety of evidence has accumulated over the past several decades indicating that the heart develops similarly in all species. Furthermore, it is apparent that many congenital abnormalities in adult hearts will likely be best understood by studying the embryonic development phases of cardiac tissue (reviewed in Harvey and Rosenthal, 1998). Thus, we endeavored to build on earlier studies which helped define the conditions for optimal cardiogenesis in the model vertebrate organism, *Xenopus*.

Grunz (1992) succeeded in producing beating hearts *in vitro* by treating isolated *Xenopus* dorsal lips with Suramin, a polyanionic compound. The Suramin-treated dorsal lips formed secondary heart structures in the ectopic transplantation and acted as a substitute for the original heart in the replacement transplantation experiment (Grunz, 1999). In *Xenopus* early development, the heart primordia differentiate into hearts under the influence of the adjacent endoderm and dorsal lip (Nascone and Melcora, 1995). Neural tissues act in a negative fashion on this inductive interaction. Suramin is likely to change the fate of the dorsal lips from dorsal mesoderm to heart and suppress their neural inducing activity. Therefore, the heart differentiation of the Suramin-treated dorsal lip contains a complex and multi-step process, which is disadvantageous for analyzing the molecular mechanism of cardiogenesis *in vitro*, especially the earliest phase of the inductive interaction. In addtion, we previously reported the urodele newt animal caps developed into beating hearts by treating with a high concentration of activin (Ariizumi *et al.*, 1996). Approximately 30% of the animal caps formed beating hearts and the rate of formation reached 50% when they were co-cultured with intact animal caps. Those percentages were also imperfect as a model system for analyzing heart development *in vitro*. Thus, we embarked on the development of a more suitable system using *Xenopus* pluripotent cells that would be more advantageous to molecular biological analysis.

The data generated in this study provide a research platform for further analysis of cardiac development. Important features of this model system include the following: First, this heart induction system, using blastula-stage pluripotent cells, represents a simple yet reliable method that can be quickly and inexpensively exploited by a broad range of researchers. Most previous studies, especially those with mammalian embryos, have been undertaken with the burden of isolating the primordia from embryos, which are difficult to obtain and which require special expertise for the dissection and isolation of heart primordia. In the protocol described herein, the key step is the dissociation/reaggregation procedure, which is straightforward and readily accomplished. Whether activin itself is the actual inducer remains uncertain (Logan and Mohun, 1993; Schneider and Mercola, 2001). Most probably activin, especially at the relatively high concentrations employed in this culture system, is involved in a complex regulatory circuit that may include other peptide growth factors (e.g., BMP, FGF, etc.) functioning in the "induction" process (Lough *et al.*, 1996; Schultheiss *et al.*, 1997; Barron *et al.*, 2000; Shi *et al.*, 2000). Wnt signals, which likely act in both a positive (Pandur *et al.*, 2002) and a negative (Schneider and Mercola, 2001; Marvin *et al.*, 2001) fashion, also participate in the induction process. With this model system it should be possible to elucidate many of the details of the regulatory circuits, especially those involved in the earliest stages of the induction process (Lohr and Yost, 2000; Zaffran and Frasch, 2002).

Second, the demonstration that ectopic transplants develop sufficiently to participate in the development of the blood vascular system opens further avenues for experimentation. The transplanted heart primordium developed an atrium and ventricle connected with the host's blood vessels. To date we have not, however, succeeded in completely replacing the original heart with a transplanted primordium. Further improvement of the transplantation protocol (e.g., changing the stage at which transplantation is performed) will probably be the key to success. Since the fundamental mechanisms of heart development are evolutionarily conserved among vertebrates (Lyons, 1996; Mohun and Sparrow, 1997), the simple amphibian system described herein warrants exploitation, especially as a model for organ engineering.

Experimental Procedures

Embryos and activin solution

Embryos of the African clawed frog, *Xenopus laevis*, were obtained using standard procedures (Ariizumi *et al.*, 1999) and staged according to Nieuwkoop and Faber (1956). Holtfreter's saline (HS; 60 mM NaCl, 0.7 mM KCl, 0.9 mM $CaCl_2$, 4.6 mM HEPES, 0.1 g/l kanamycin sulfate, 0.1% BSA [A-7888, Sigma, USA], pH 7.6) was used as a medium in all experiments. A peptide growth factor, human recombinant activin A (a gift from Dr. Y. Eto [Central Research Laboratories, Ajinomoto Co. Inc., Japan]), was used as an inducer and dissolved in HS at appropriate concentrations (10-1,000 ng/ml).

In vitro *heart induction protocol*

The animal cap region was squarely removed from the mid-blastula stage embryo (st. 8) using tungsten needles. It was 0.8 mm x 0.8 mm in size and contained 205 ± 32 cells (n = 10). The following procedure, named the dissociation/reaggregation protocol, was performed in 96-well plates with round bottoms (SUMILON; MS-309UR, Sumitomo Bakelite, Japan). A maximum of 10 animal caps were bathed in 100 µl of Ca^{2+}-free HS for 20 min to loosen their cell adhesion. After being exchanged for 100 µl of activin solution (e.g., 100 ng/ml, dissolved in HS containing Ca^{2+}), cells were dispersed by gentle pipetting. The newly formed spherical reaggregates were transferred into 200 µl of HS after they had been left in the activin solution for a defined period (e.g., 5 h).

In vivo *heart transplantation protocol*

After being precultured in HS for 1 day, the reaggregate prepared as described above was divided into small pieces and transplanted as a donor tissue into the sibling neurulae (st. 20). In replacement transplantation, the original heart primordium (with the surrounding epidermis) of the host embryo was replaced with a fragment of reaggregate. In ectopic transplantation, a donor fragment was inserted into a slit made in the host's abdomen. The transplanted embryos were kept in 10% HS for the first 4 days, and raised in dechlorinated water until they metamorphosed to adults. To trace the lineage of donor tissue in the transplanted embryos, embryos were injected at the two-cell stage with a total volume of 10 nl of 1% fluorescein-dextran-amine (FDA; D-1820, Molecular Probes, USA) or 1% Texas Red-dextran-amine (TRDA; D-1863, Molecular Probes, USA). Animal caps dissected from TRDA-labeled blastulae were used for making donor heart rudiments, while FDA-labeled neurulae were used as recipients. The 4-day-old larvae were examined under an epifluorescence microscope. Fluorescent photographic images were computer-composed using photo-retouching software.

Gene expression analyses and histology

Whole-mount *in situ* hybridization was performed according to Harland (1991). Probes were generated using DIG RNA labeling mixture (Boehringer Mannheim) and color was developed by BCIP/NBT. In the RT-PCR analysis, total RNA isolation and RT-PCR were performed as previously described (Yokota *et al.*, 1998). Sequences of the oligonucleotide primers are available

from the authors on request. Transplanted embryos and ectopic hearts were fixed in Bouin's fluid for 12 h, dehydrated in a graded series of ethanol, cleared in xylene, embedded in paraffin, and cut into 8-μm thick sections. Sections were stained with Delafield's hematoxylin/eosin.

Acknowledgements

This work was supported in part by Grants-in-Aid for Scientific Research from the Ministry of Culture, Sports, Science and Technology of Japan, and by SORST (Solution Oriented Research for Science and Technology) of the Japan Science and Technology Corporation.

Electronic Supplementary Material for this paper, consisting of four "QuickTime" movies is available at the following address: http://www.ijdb.ehu.es/abstract.0306/esm1.htm

Supplementary Movie 1. An *in vitro*-induced beating heart. Animal cap tissues developed into beating hearts after combined activin and dissociation/reaggregation treatments. These induced hearts kept beating rhythmically for more than 2 weeks without a change in the culture medium.

Supplementary Movie 2. A tadpole with a secondary heart (ventral view). The recipient neurula embryo developed into a tadpole with a double heart after the ectopic transplantation of the *in vitro*-induced heart rudiment. The ectopic heart of this 5-day-old tadpole is filled with a large number of red blood cells.

Supplementary Movie 3. An adult frog with a secondary heart. This frog was ectopically transplanted with an *in vitro*-induced heart rudiment at the neurula stage. The recipient embryo metamorphosed into a frog normally except for exhibiting an ectopic beating heart.

Supplementary Movie 4. Internal anatomy of a frog with an ectopic heart. This frog is the same as shown in Fig. 3F. When the host's anterior abdominal vein was clamped the ectopic heart expanded with a large amount of blood.

References

ARIIZUMI, T. and ASASHIMA, M. (2001). *In vitro* induction systems for analyses of amphibian organogenesis and body patterning. *Int. J. Dev. Biol.* 45: 273-279.

ARIIZUMI, T., SAWAMURA, K., UCHIYAMA, H. and ASASHIMA, M. (1991). Dose and time-dependent mesoderm induction and outgrowth formation by activin A in *Xenopus laevis*. *Int. J. Dev. Biol.* 35: 407-414.

ARIIZUMI, T., KOMAZAKI, S., ASASHIMA, M. and MALACINSKI, G.M. (1996). Activin treated urodele ectoderm: a model experimental system for cardiogenesis. *Int. J. Dev. Biol.* 715-718.

ARIIZUMI, T., TAKANO, K., ASASHIMA, M. and MALACINSKI, G.M. Bioassays of inductive interactions in amphibian development. *Method in Molecular Biology, Vol. 135: Developmental Biology Protocols, Vol. I* (eds. Tuan, R.S. and Lo, C.W.) 89-112 (Humana Press, Totawa, NJ, 1999).

ASASHIMA, M., NAKANO, H., SHIMADA, K., KINOSHITA, K., ISHII, K., SHIBAI, H., and UENO, N. (1990). Mesodermal induction in early amphibian embryos by activin A (erythroid differentiation factor). *Roux's Archives Develop.Biol.* 198: 330-335.

ASASHIMA, M., KINOSHITA, K., ARIIZUMI, T. and MALACINSKI, G.M. (1999). Role of activin and other peptide growth factors in body patterning in the early amphibian embryo. *Int. Rev. Cytol.* 191: 1-52.

BARRON, M., GAO, M. and LOUGH, J. (2000). Requirement for BMP and FGF signaling during cardiogenic induction in non-precardiac mesoderm is specific, transient, and cooperative. *Dev. Dyn.* 218: 383-393.

CHAN, T.C., ARIIZUMI, T. and ASASHIMA, M. (1999). A model system for organ engineering: transplantation of *in vitro* induced embryonic kidney. *Naturwissenschaften* 86: 224-227.

DRYSDALE, T.A., TONISSEN, K.F., PATTERSON, K.D., CRAWFORD, M.J. and KRIEG, P.A. (1994). *Cardiac troponin I* is a heart-specific marker in the *Xenopus* embryo: expression during abnormal heart morphogenesis. *Dev. Biol.* 165: 432-441.

GRUNZ, H. (1992). Suramin changes the fate of Spemann's organizer and prevents neural induction in *Xenopus* laevis. *Mech. Dev.* 38: 133-141.

GRUNZ, H. (1999). Amphibian embryos as a model system for organ engineering: *in vitro* induction and rescue of the heart anlage. *Int. J. Dev. Biol.* 43: 361-364.

HARLAND, R.M. (1991). *In situ* hybridization: an improved whole-mount method for *Xenopus* embryos. *Methods Cell Biol.* 36: 685-695.

HARBEY, R.P., and ROSENTHAL, N., eds. (1998). Heart Development. Academic Press, New York.

HORB, M.E. and THOMSEN, G.H. (1999). *Tbx5* is essential for heart development. *Development* 126: 1739-1751.

JIANG, Y. and EVANS, T. (1996). The *Xenopus GATA-4/5/6* genes are associated with cardiac specification and can regulate cardiac-specific transcription during embryogenesis. *Dev. Biol.* 174: 258-270.

LOGAN, M. and MOHUN, T. (1993). Induction of cardiac muscle differentiation in isolated animal pole explants of *Xenopus laevis* embryos. *Development* 118: 865-875.

LOHR, J.L. and YOST, H.J. (2000). Vertebrate model systems in the study of early heart development: *Xenopus* and zebrafish. *Am. J. Med. Genet.* 97: 248-257.

LOUGH, J., BARRON, M., BROGLEY, M., SUGI, Y., BOLENDER, D.L. and ZHU, X. (1996). Combined BMP-2 and FGF-4, but neither factor alone, induces cardiogenesis in non-precardiac embryonic mesoderm. *Dev. Biol.* 178: 198-202.

LYONS, G.E. (1996). Vertebrate heart development. *Curr. Opin. Genet. Dev.* 6: 454-460.

MARVIN, M.J., DI ROCCO, G., GARDINER, A., BUSH, S.M. and LASSAR, A.B. (2001). Inhibition of Wnt activity induces heart formation from posterior mesoderm. *Genes Dev.* 15: 316-327.

MOHUN, T. and SPARROW, D. (1997). Early steps in vertebrate cardiogenesis. *Curr. Opin. Genet. Dev.* 7, 628-633.

NASCONE, N. and MERCOLA, M. (1995). An inductive role for the endoderm in *Xenopus* cardiogenesis. *Development* 121: 515-523.

NIEUWKOOP, P.D. and FABER, J. *Normal Table of Xenopus laevis (Daudin).* (North Holland, Amsterdam, 1956).

PANDUR, P., LÄSCHE, M., EISENBERG, L.M. and KÜHL, M. (2002). Wnt-11 activation of a non-canonical Wnt signaling pathway is required for cardiogenesis. *Nature* 418: 636-641.

SCHNEIDER, V.A. and MERCOLA, M. (2001). Wnt antagonism initiates cardiogenesis in *Xenopus laevis*. *Genes Dev.* 15: 304-315.

SCHULTHEISS, T.M., BURCH, J.B. and LASSAR, A.B. (1997). A role for bone morphogenetic proteins in the induction of cardiac myogenesis. *Genes Dev.* 11: 451-462.

SHI, Y., KATSEV, S., CAI, C. and EVANS, S. (2000). BMP signaling is required for heart formation in vertebrates. *Dev. Biol.* 224: 226-237.

SMALL, E.M. and KRIEG, P.A. (2000). Expression of *atrial natriuretic factor (ANF)* during *Xenopus* cardiac development. *Dev. Genes Evol.* 210: 638-640.

TONISSEN, K.F., DRYSDALE, T.A., LINTS, T.J., HARVEY, R.P. and KRIEG, P.A. (1994). *XNkx-2.5*, a *Xenopus* gene related to *Nkx-2.5* and *tinman*: evidence for a conserved role in cardiac development. *Dev. Biol.* 162: 325-328.

YOKOTA, C., TAKAHASHI, S., EISAKI, A., ASASHIMA, M., AKHTER, S., MURAMATSU, T. and KADOMATSU, K. (1998). Midkine counteracts the activin signal in mesoderm induction and promotes neural formation. *J. Biochem. (Tokyo)* 123: 339-346.

ZAFFRAN, S. and FRASCH, M. (2002). Early signals in cardiac development. *Circ. Res.* 91: 457-469.

Received: July 2003
Reviewed by Referees: August 2003
Modified by Authors and Accepted for Publication: August 2003
Edited by: Makoto Asashima

Selective Involvement of p130Cas/Crk/Pyk2/c-Src in Endothelin-1–Induced JNK Activation

Hiroaki Kodama, Keiichi Fukuda, Eiichi Takahashi, Satoko Tahara, Yuichi Tomita, Masaki Ieda, Kensuke Kimura, Koji M. Owada, Kristiina Vuori, Satoshi Ogawa

Abstract—Both integrin-based focal adhesion complexes and receptor tyrosine kinases have been proposed as scaffolds on which the G protein–coupled receptor (GPCR)–induced signaling complex might assemble. We have recently reported that Ca^{2+}-sensitive tyrosine kinase, Pyk2, and epidermal growth factor receptor (EGFR) act as independently regulated scaffolds in cardiomyocytes. In this report, we investigated the activation and regulation of p130Cas, Crk, Pyk2, and c-Src by a well-known hypertrophic agonist, endothelin-1 (ET), and determined their contributions to the activation of c-Jun NH_2-terminal kinase (JNK) and extracellular signal–regulated kinase (ERK) in cardiomyocytes. Like Pyk2, ET-induced tyrosine phosphorylation of p130Cas was significantly inhibited by either chelating intracellular Ca^{2+} ($[Ca^{2+}]_i$) or a protein kinase C inhibitor, calphostin C. This activation of p130Cas was also abrogated by the tetrapeptide RGDS, which disrupts integrin heterodimerization; cytochalasin D, which depolymerizes the actin cytoskeleton; or a selective Src family kinase inhibitor, PP2, but not by an EGFR inhibitor, AG1478. We also observed ET-induced temporal associations of Pyk2 with active c-Src, followed by p130Cas with Pyk2, c-Src, and Crk. Overexpression of a dominant-negative mutant of p130Cas (CasΔSD), Crk (CrkSH2m), Pyk2 (PKM), or *C*-terminal Src kinase (Csk), but not of a deletion mutant of EGFR (533delEGFR), attenuated ET-induced JNK activation. Similarly, an ET-induced increase in c-*jun* promoter luciferase activity was inhibited by overexpression of CasΔSD, CrkSH2m, PKM, or Csk. In contrast, ET-induced ERK activation and c-*fos* gene expression were predominantly regulated by EGFR. Collectively, the focal adhesion–dependent p130Cas/Crk/Pyk2/c-Src–mediated pathway is selectively involved in ET-induced JNK activation in cardiomyocytes. (***Hypertension.* 2003;41:1372-1379.**)

Key Words: endothelin-1 ■ cardiac hypertrophy ■ kinase ■ focal adhesion ■ phosphorylation

Cardiac hypertrophy is characterized by both remodeling of the extracellular matrix (ECM) and the hypertrophic growth of cardiomyocytes.[1] Focal adhesions are regions of a cell in direct contact with the ECM, providing anchorage sites linking the ECM to the actin cytoskeleton by way of the integrin family of cell-surface receptors.[2,3] The ECM can regulate reorganization of the cytoskeletal architecture, and ECM-mediated signaling has also been implicated in the growth factor–induced alterations of gene transcription in cardiomyocytes.[4] Mitogen-induced changes in the actin cytoskeleton are accompanied by dramatic changes in several proteins present in focal adhesions.

A 130-kDa Crk-associated substrate, p130Cas, was originally identified as a protein highly tyrosine-phosphorylated in cells transformed by v-Src and v-Crk oncogenes.[5] Molecular cloning of p130Cas revealed a docking protein that contains an SH3 domain, proline-rich regions, and a cluster of 15 putative SH2-binding motifs.[6] This unique structure of p130Cas suggests a role in assembling multiprotein signaling complexes.[7] Indeed, p130Cas localizes to focal adhesions and associates not only with focal adhesion proteins, such as focal adhesion kinases (FAK) and paxillin, but also with other SH2 domain–containing signaling molecules, including Crk.[7,8] p130Cas is also phosphorylated during cell adhesion or after stimulation with various growth factors, such as angiotensin II,[9] platelet-derived growth factor, and endothelin-1 (ET).[10]

One of the prime candidates of tyrosine kinase responsible for p130Cas activation is Pyk2,[8,11] a close relative of FAK. Moreover, Pyk2 has been shown to be responsible for linking c-Src to downstream signaling pathways, such as the activation of extracellular signal–regulated kinases (ERKs)[11,12] and c-Jun NH_2-terminal kinases (JNKs).[13] Recent studies also suggest that the activation of p130Cas is critical in cardiac development, because targeted disruption of the p130Cas gene led to an impaired cardiovascular system demonstrating marked systemic congestion and a poorly developed heart.[14]

Among the many signaling molecules that are activated by hypertrophic stimuli, members of the mitogen-activated pro-

Received August 5, 2002; first decision August 21, 2002; revision accepted March 20, 2003.

From the Cardiopulmonary Division, Department of Internal Medicine (H.K., K.F., E.T., S.T., Y.T., M.I., K.K., S.O.), and the Institute for Advanced Cardiac Therapeutics (K.F.), School of Medicine, Keio University, Tokyo, Japan; the Institute of Molecular and Cellular Biology for Pharmaceutical Sciences, Kyoto Pharmaceutical University (K.M.O.), Kyoto, Japan; and the La Jolla Cancer Research Center, Burnham Institute (K.V.), La Jolla, Calif.

Correspondence to Keiichi Fukuda, MD, PhD, Cardiopulmonary Division, Department of Internal Medicine, School of Medicine, Keio University, 35 Shinanomachi, Shinjuku-ku, Tokyo 160-8582, Japan. E-mail kfukuda@sc.itc.keio.ac.jp

Hypertension is available at http://www.hypertensionaha.org DOI: 10.1161/01.HYP.0000069698.11814.F4

tein kinase (MAPK) family, including ERK, JNK, and p38 MAPK, are likely to play an important role in cardiac hypertrophic gene expression.[15] However, very little is known about the signals downstream of focal adhesion proteins, including p130Cas, Crk, and Pyk2, which mediate selective activation of the JNK pathway in contrast to the ERK pathway in cardiomyocytes.

In a previous report, we showed that ET activated the 2 distinct tyrosine kinase pathways requiring Pyk2 or epidermal growth factor receptor (EGFR) in cardiomyocytes. EGFR was Ca^{2+}-independently activated, recruited Shc, and predominantly contributed to ERK/c-*fos* activation, whereas Pyk2 or c-Src contributed less to ERK activation.[16] We show here that $[Ca^{2+}]_i$, PKC, c-Src, and focal adhesion integrity are also required for ET-induced tyrosine phosphorylation of p130Cas as well as Pyk2. Furthermore, we demonstrate that ET-induced JNK activation is preferentially regulated by Pyk2, c-Src, and the p130Cas/Crk complex but not by EGFR. Thus, the p130Cas/Crk/Pyk2/c-Src-JNK signaling described here might represent a pathway clearly dissociable from the EGFR-mediated ERK cascade in cardiomyocytes.

Methods

Materials

PP2, AG1478, and AG490 were purchased from Calbiochem. ET, myelin basic protein (MBP), calphostin C, phorbol 12-myristate 13-acetate (PMA), BAPTA, BQ123, A23187, RGDS, and cytochalasin D were purchased from Sigma.

Cell Culture and Transfection

Primary cultured cardiomyocytes were prepared from ventricles of 1-day-old neonatal Wistar rats as described previously.[16] Hemagglutinin (HA)-tagged JNK1 (HA-JNK1) and HA-ERK2 were provided by E. Nishida and M. Karin, respectively. *C*-terminal Src kinase (Csk), the deletion mutant of EGFR (533delEGFR),[17] the dominant-negative mutant of Jak2 (d.n.Jak2), and the kinase-inactive mutant of Pyk2 (PKM)[11] were provided by H. Sabe, H. Matsubara, J. Ihle, and J. Schlessinger, respectively. pSSRα-p130CasΔSD (deletion of 213 to 514 amino acids; CasΔSD) and pSSRα-Crk-SH2m (Crk-SH2 R38V mutant; CrkSH2m) have been described elsewhere.[18,19] Transfection of plasmid was performed with the use of Effectene transfection reagent (Qiagen). After 24 hours of serum depletion, cells were stimulated with ET.

Luciferase Assays

pGVB −438c-*jun*-luc, containing segment −438 to +140 of the rat c-*jun* promoter[20] (c-*jun*-luc), and pGL3-c-*fos*p, containing segment −404 to +41 of the human c-*fos* promoter[21] (c-*fos*-luc), were provided by S. Hata and M. Tsuda, respectively. For each dish, 0.4 μg c-*jun*-luc or c-*fos*-luc together with 2.0 μg CasΔSD, CrkSH2 m, 533delEGFR, Csk, PKM, or d.n.Jak2 were transfected into cardiomyocytes. Cell lysates were processed and assayed for luciferase activity with a luciferase assay system (Promega).

Immunoprecipitation and Immunoblotting

Immunoprecipitation was performed with monoclonal anti-p130Cas and anti-Crk (Transduction Laboratories); polyclonal anti-JNK1, anti-Pyk2, anti–c-Src (SRC2), and anti-EGFR antibodies (Santa Cruz Biotechnology); or monoclonal anti-HA antibodies (Roche Molecular Biochemicals), as described previously.[16] For immunoblot analysis, immunoprecipitates were subjected to sodium dodecyl sulfate–polyacrylamide gel electrophoresis (SDS-PAGE) and then transferred to nitrocellulose membranes. The blots were incubated with anti-phosphotyrosine (4G10), anti-p130Cas, anti-Crk, or monoclonal anti–c-Src (clone 28) antibody, which selectively recognizes the active (Tyr-530–dephosphorylated) form of c-Src.[22] Signals were detected by enhanced chemiluminescence (Amersham).

Kinase Assay of JNK and ERK

JNK and ERK activities were determined by in vitro kinase reactions, as described previously.[16] In brief, JNK1 or ERK2 immunoprecipitates were incubated with glutathione S-transferase (GST)–c-Jun(1-79) for 30 to 45 minutes at 30°C or with MBP for 10 minutes at 25°C. After SDS-PAGE, the gels were dried and subjected to autoradiography. The GST–c-Jun(1-79) construct was provided by M. Hibi.[23]

Reproducibility of Results and Statistical Analysis

Unless stated otherwise, the results are representative of at least 3 separate experiments that gave similar results. Densitometric analysis was performed with Image J, version 1.6. The significance of differences among mean values was determined by ANOVA.

Results

p130Cas Is Tyrosine-Phosphorylated on Cell Adhesion in a Ca^{2+}-, PKC-, and c-Src–Dependent Manner

We first examined the kinetics of tyrosine phosphorylation of p130Cas. As shown in Figure 1A, ET stimulated tyrosine phosphorylation of p130Cas, with peak phosphorylation occurring at 5 minutes. Tyrosine phosphorylation remained above basal levels at 30 minutes. This p130Cas tyrosine phosphorylation was significantly inhibited by pretreatment with the ET-A receptor blocker BQ123, thus suggesting that p130Cas tyrosine phosphorylation was mediated by the ET-A receptor (Figure 1B).

We next studied the dependence of ET-induced p130Cas phosphorylation on changes in $[Ca^{2+}]_i$ or activation of protein kinase C (PKC). ET stimulation causes rapid activation of PKC and an elevation of $[Ca^{2+}]_i$ in cardiomyocytes.[24] Direct stimulation of PKC by PMA or Ca^{2+} ionophore A23187 caused p130Cas tyrosine phosphorylation (Figure 1C). On the other hand, either the chelation of $[Ca^{2+}]_i$ or the inhibition of PKC by calphostin C significantly suppressed the ET-induced p130Cas tyrosine phosphorylation (Figure 1D). These results suggest that activation by both $[Ca^{2+}]_i$ and PKC is required for p130Cas tyrosine phosphorylation in cardiomyocytes.

Because p130Cas colocalizes with Pyk2 or paxillin to the focal adhesion plaques,[25] it has been suggested that p130Cas might be involved in cytoskeletal signaling, dependent on the proper assembly of focal adhesions.[3] The tetrapeptide RGDS, which disrupts integrin heterodimerization,[26] or cytochalasin D, which depolymerizes the actin cytoskeleton,[9,26] fully prevented the ET-induced p130Cas phosphorylation (Figure 1E), thus suggesting that the integrity of the cardiomyocyte cytoskeleton is required for ET-induced p130Cas tyrosine phosphorylation.

ET is known to activate various tyrosine kinases, including c-Src, EGFR, and Jak2.[16,27] To characterize the tyrosine kinase responsible for p130Cas phosphorylation by ET, we used selective tyrosine kinase inhibitors; AG1478, an EGFR inhibitor; PP2, a Src family kinase inhibitor;[9,27] and AG490, a Jak2 inhibitor. PP2 abolished ET-induced p130Cas tyrosine phosphorylation, whereas AG1478 or AG490 had no effect, thus suggesting that activation of c-Src might lie upstream of p130Cas in ET-induced signaling (Figure 1F).

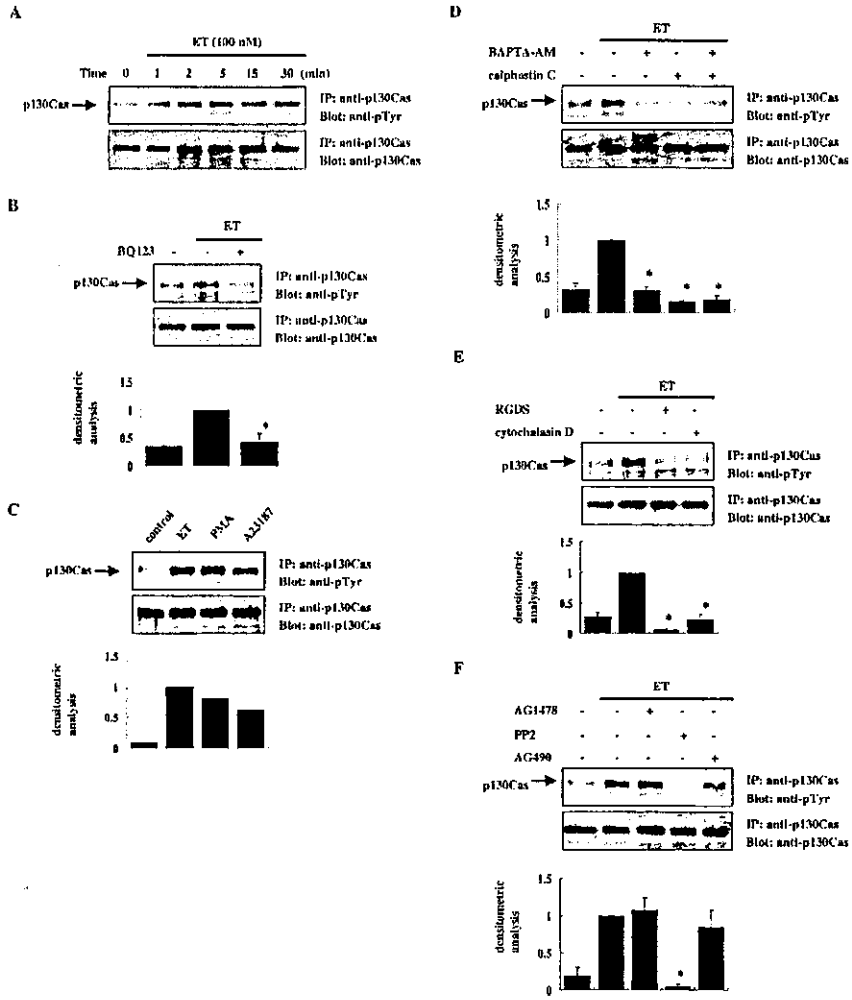

Figure 1. ET-induced tyrosine phosphorylation of p130Cas is dependent on focal adhesion, PKC, Ca^{2+}, and c-Src in cardiomyocytes. A, Cells were stimulated with ET (100 nmol/L) for the indicated times. p130Cas was immunoprecipitated (IP) with anti-p130Cas monoclonal antibody (mAb) and immunoblotted (Blot) with an anti-phosphotyrosine (pTyr) mAb. The same membrane was immunoblotted with an anti-p130Cas mAb to confirm the equal expression of p130Cas. B, Cells were pretreated with or without BQ123 (2 μmol/L) for 30 minutes and stimulated with ET (100 nmol/L) for 15 minutes. C, Cells were left unstimulated (control) or stimulated with ET (100 nmol/L), PMA (1 μmol/L), or A23187 (10 μmol/L) for 15 minutes. D, Cells were pretreated with BAPTA-AM (50 μmol/L) for 30 minutes or calphostin C (1 μmol/L) for 1 hour and stimulated with ET (100 nmol/L) for 15 minutes. E, Cells were pretreated with vehicle (−, DMSO), RGDS (1 mmol/L) overnight, or cytochalasin D (10 μmol/L) for 30 minutes and stimulated with ET. F, Cells were pretreated with vehicle (−, DMSO), AG1478 (250 nmol/L), PP2 (50 μmol/L), or AG490 (20 μmol/L) for 30 minutes and stimulated with ET. All data were quantified by densitometric analysis and expressed as the fold increase compared with ET-stimulated cells (lower panel). *$P<0.05$, significant difference compared with ET-stimulated cells.

p130Cas Forms Temporal Associations With Pyk2, Active c-Src, and Crk in Response to ET

The protein sequence of p130Cas suggests that it might serve as an adapter protein, and p130Cas is thought to recruit cytoskeletal signaling molecules or other SH2 domain–containing molecules.[6,7] We attempted to identify some of the proteins that were observed in p130Cas or Pyk2 immune-complex assays. ET induced a rapid, temporal association of Pyk2 with active c-Src as early as 1 minute (Figure 2A), and thereafter the autokinase activity of Pyk2 gradually increased, peaked at 5 minutes, and then returned to near basal levels at 60 minutes (Figure 2B). After Pyk2 binds to SH2 domains of Src family tyrosine kinases, c-Src is then known to phosphorylate several other sites in Pyk2, which in turn function as binding sites for signaling molecules containing SH2 domains.[12] We next observed that ET increased a transient association of Pyk2 with p130Cas after the increased autokinase activity of Pyk2 (Figure 2C). ET also increased the association of p130Cas with active c-Src (Figure 2D). Moreover, ET enhanced the association of p130Cas with Crk (Figure 2E).

ET-Induced JNK Activation Requires Both Ca^{2+} and PKC and a c-Src–Dependent Signal in Cardiomyocytes

Kudoh et al[28] reported that G protein–coupled receptor (GPCR) stimulation by angiotensin II activated JNK in cardiomyocytes and that the activation of JNK was suppressed by downregulation of PKC or by chelating $[Ca^{2+}]_i$. We confirmed that another GPCR ligand, ET, activated JNK in a time-dependent manner, and ET-induced JNK activation was significantly attenuated by chelating $[Ca^{2+}]_i$ or by calphostin C (Figures 3A and 3B).

Furthermore, JNK activation was abrogated by PP2, whereas AG1478 or AG490 had no effect (Figure 3C). The results of the inhibitory effect of PP2 suggested that Src family kinases were selectively involved in the activation of JNK. Either RGDS or cytochalasin D significantly inhibited JNK activation (Figure 3D). Because activation of p130Cas or Pyk2[16] is also dependent on PKC, $[Ca^{2+}]_i$, and c-Src, it is possible to speculate that JNK activation by ET might be at least partly mediated through the focal adhesion proteins p130Cas or Pyk2 associated with c-Src.

CasΔSD, CrkSH2m, Pyk2, or Csk Significantly Inhibits ET-Induced Activation of JNK but Not of ERK

To confirm that the p130Cas/Crk complex or Pyk2 is critically involved in ET-induced JNK activation, we transfected the cells with HA-JNK1 or HA-ERK2, together with CasΔSD, CrkSH2m, 533delEGFR, Csk, PKM, or d.n.Jak2

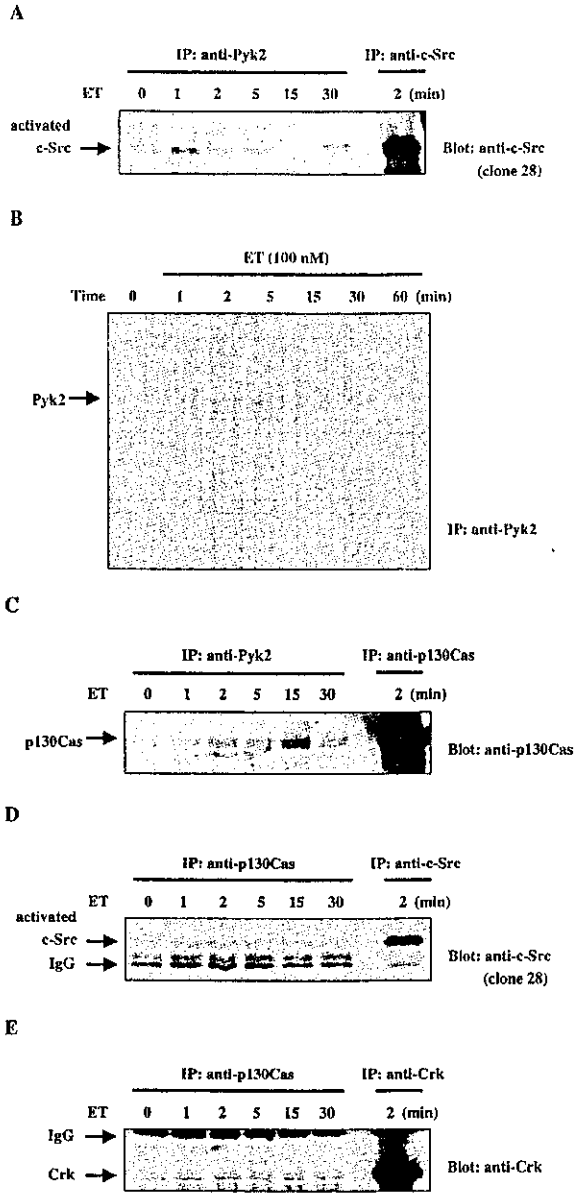

Figure 2. ET augmented p130Cas protein/protein complex formation. Cells were stimulated with ET (100 nmol/L) for the indicated times. A, Pyk2 or c-Src was immunoprecipitated (IP) with an anti-Pyk2 polyclonal antibody (pAb) or an anti-c-Src (SRC2) pAb and immunoblotted (Blot) with an anti-c-Src (clone 28) monoclonal antibody (mAb). B, Pyk2 was immunoprecipitated with an anti-Pyk2 pAb and incubated with γ-[^{32}P]ATP for 30 minutes. After SDS-PAGE, the gels were dried and subjected to autoradiography. C, Pyk2 or p130Cas was immunoprecipitated with an anti-Pyk2 pAb or an anti-p130Cas mAb and immunoblotted with an anti-p130Cas mAb. D, p130Cas or c-Src was immunoprecipitated with an anti-p130Cas pAb or an anti-c-Src (SRC2) pAb and immunoblotted with anti-c-Src (clone 28). E, p130Cas or Crk was immunoprecipitated with an anti-p130Cas pAb or an anti-Crk mAb and immunoblotted with an anti-Crk mAb.

and stimulated them with ET. Overexpression of CasΔSD or CrkSH2m had been previously shown to interfere with p130Cas/Crk signaling.[18] ET-induced JNK activation was strongly attenuated by CasΔSD, CrkSH2m, Csk or PKM, but it was not noticeably inhibited by 533delEGFR or d.n.Jak2

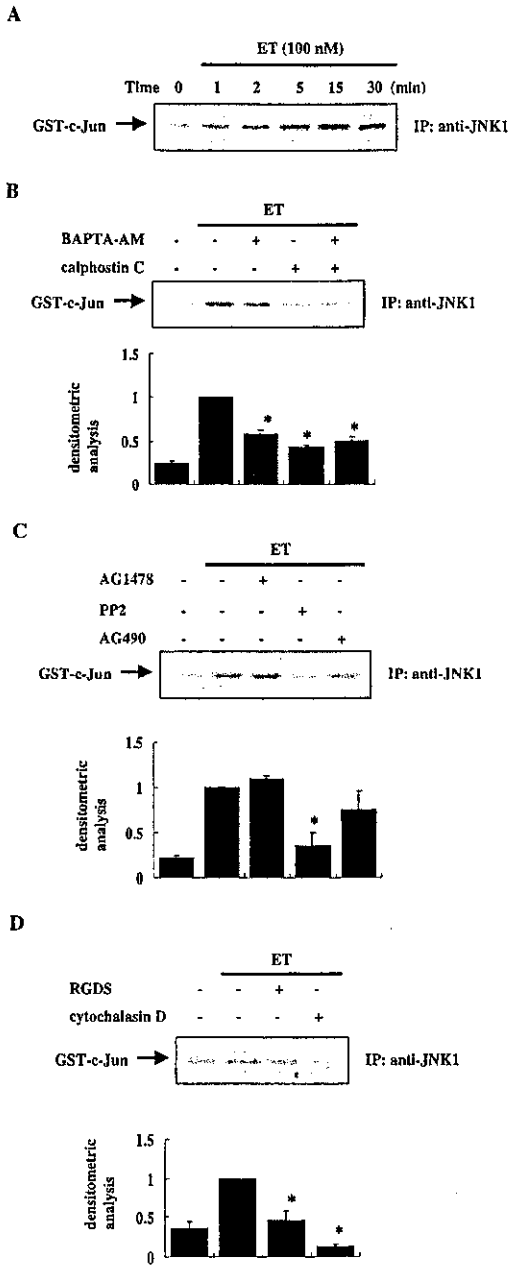

Figure 3. ET-induced activation of JNK required both Ca^{2+} and PKC and c-Src. A, Cells were stimulated with ET (100 nmol/L) for the indicated times. JNK1 was immunoprecipitated (IP) with an anti-JNK1 polyclonal antibody and incubated with GST-c-Jun(1-79) as a substrate. The immunoprecipitates were electrophoresed and subjected to autoradiography. B, Cells were pretreated with BAPTA-AM (50 μmol/L) for 30 minutes or calphostin C (1 μmol/L) for 1 hour and stimulated with ET (100 nmol/L) for 15 minutes. C, Cells were pretreated with vehicle (−, DMSO), AG1478 (250 nmol/L), PP2 (50 μmol/L), or AG490 (20 μmol/L) for 30 minutes and stimulated with ET. D, Cells were pretreated with vehicle (−, DMSO), RGDS (1 mmol/L) overnight, or cytochalasin D (10 μmol/L) for 30 minutes and stimulated with ET. The amount of ^{32}P incorporated into GST-c-Jun(1-79) was determined by densitometry. Graph indicates the fold increase in JNK activity relative to values obtained in ET-stimulated cells (lower panel). Shown is the mean±SD, n=4, *P<0.05.